Russian Chemical Reviews **84** (5) 455–484 (2015) © 2015 Russian Academy of Sciences and Turpion Ltd

DOI 10.1070/RCR4445

Electronic structure, aromaticity and spectra of hetero[8]circulenes

G V Baryshnikov,[a] B F Minaev,[a, b] V A Minaeva [a]

[a] Cherkasy National University named after Bohdan Khmelnitsky
bulv. Shevchenko 81, 18031 Cherkasy, Ukraine
[b] National Research Tomsk State University
prosp. Lenina 36, 634050 Tomsk, Russian Federation

The present review highlights recent advances in experimental and theoretical chemistry dealing with investigation of the electronic structures and physicochemical properties of hetero[8]circulenes. These compounds are the only representatives of planar heteroannulated cyclooctatetraenes. It is shown that high molecular symmetry of hetero[8]circulenes and the extended specific π-conjugated chain are the main factors responsible for high stability of the crystal packing modes and the optical and magnetic properties of these compounds. These effects also determine numerous selection rules for electronic and vibrational transitions in UV-Vis, IR and Raman spectra. Emphasis is given to the aromaticity of hetero[8]circulenes containing the inner antiaromatic cyclooctatetraene core. The planar structure of the latter is stabilized by a polyaromatic system composed of benzene rings and five-membered heterocycles. Due to high thermal and chemical stability of most hetero[8]circulenes combined with semiconducting properties, these compounds can be considered as promising materials for molecular electronics and nanophotonics, in particular for the production of organic light-emitting diodes and field-effect transistors.
The bibliography includes 154 references.

Contents

I. Introduction 455
II. X-Ray molecular structures of hetero[8]circulenes 456
III. Crystal structures of hetero[8]circulenes 459
IV. Quantum chemical studies of the structures of hetero[8]circulenes 462
V. Spectroscopic properties of hetero[8]circulenes 466
VI. New materials based on hetero[8]circulenes 480
VII. Conclusions 481

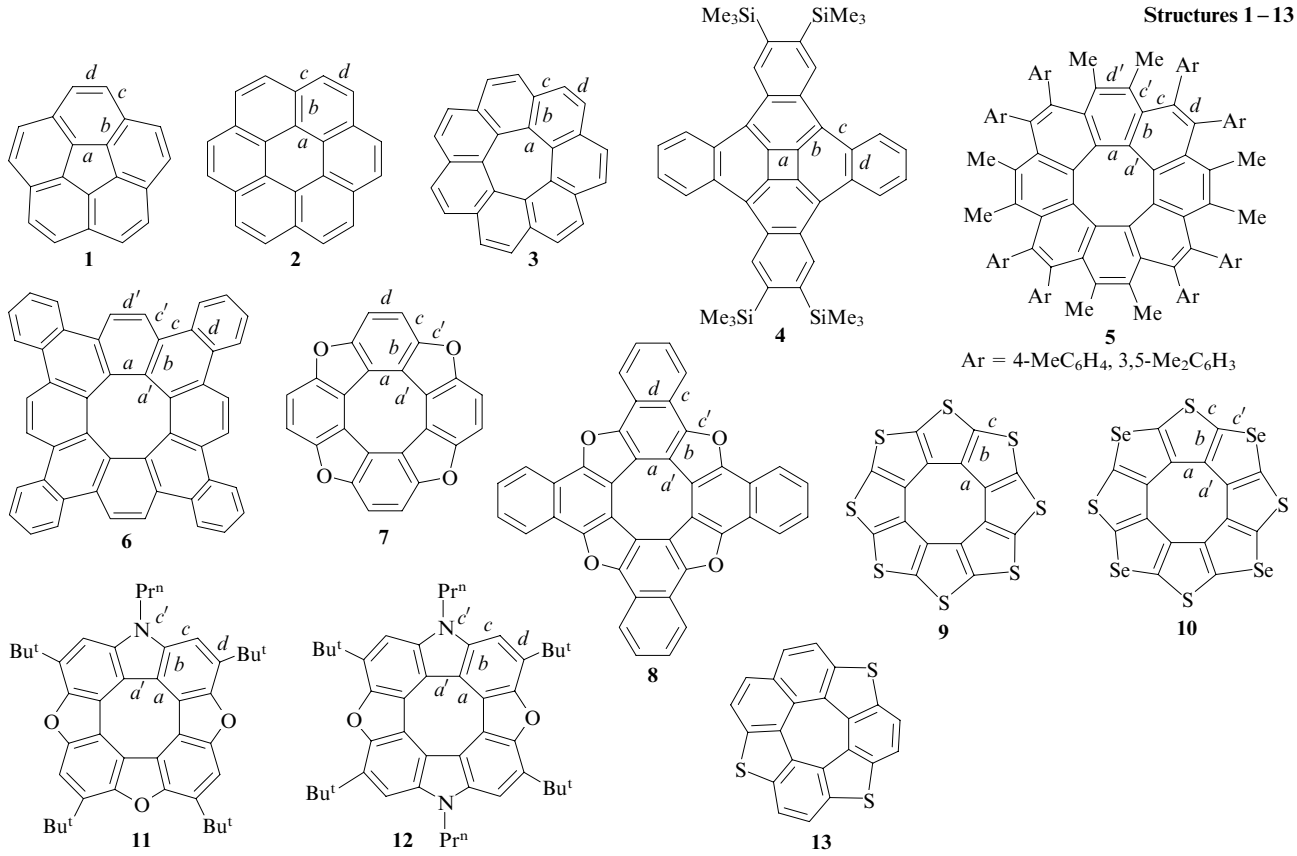
I. Introduction

Circulenes [1–4] have long drawn attention from organic chemists interested in the improvement and development of the concept of aromaticity. Hydrocarbon-type circulenes consist of benzene rings fused with each other at the bonds *a* and *c* to form an annulene macrocycle. These compounds include, in particular, well-known corannulene **1** ([5]circulene),[5] coronene **2** ([6]circulene) [6] and [7]circulene [7] **3**, as well as the recently synthesized quadrannulene **4** ([4]circulene),[8] [8]circulenes [9] **5** and tetrabenzo[8]circulene [10] **6**. These highly symmetric molecules can serve as elemental building blocks of graphene,[11–13] fullerenes [14–16] and some nanotubes,[17–19] the structural and spectroscopic properties of which were studied in detail unlike the structure-forming circulene subunits. It should be noted that studies of the chemistry

G V Baryshnikov Candidate of Chemical Sciences, Lecturer at the Chair of Organic Chemistry, Quality and Standardization of the CNU.
Telephone: +7(38-0472) 37 65 76, e-mail: glebchem@rambler.ru
Current research interests: computational quantum chemistry, chemical bonding theory, nonvalence interactions, electroluminescent materials, energy transfer mechanism in organic light-emitting diodes and dye-sensitized solar cells.
B F Minaev Doctor of Chemical Sciences, Professor, Head of the same Chair, Professor at the Chair of Optics and Spectroscopy of the NR TSU.
Telephone: +7(38-0472) 37 65 76, e-mail: bfmin@rambler.ru, boris@theochem.kth.se
Current research interests: quantum chemistry and structure of matter, spectroscopy of diatomic molecules, effects of spin–orbit coupling in chemical reactions, phosphorescence of organic compounds and complexes, theory of spin-forbidden electronic transitions.
V A Minaeva Candidate of Chemical Sciences, Associate Professor at the Chair of Chemistry of the CNU.
Telephone: +7(38-0472) 37 65 76, e-mail: minaeva@cdu.edu.ua
Current research interests: analytical chemistry, methods of concentrating inorganic compounds, chromatographic analysis, infrared and Raman spectroscopy, structure and vibrational spectra of steroid hormones.

Received 21 January 2014
Uspekhi Khimii **84** (5) 455–484 (2015); translated by T N Safonova

Structures 1–13



of circulenes substantially supplement and add details to the rapidly developing electronic structure theory and spectra of nanoassociates of sp^2-hybridized carbon.[11–18]

The term 'heterocirculenes' was proposed for the first time by Wynberg and Dopper[1] in 1972 for a new class of polyaromatic heterocyclic compounds — heterocyclic analogues of polycyclic hydrocarbon circulenes. These molecules consist of two concentric annulene rings. The inner ring has no hydrogen atoms (unlike kekulene,[2] septulene[3] and higher kekulenes[4]), and the outer ring involves heteroatoms (oxygen atoms in oxacirculenes, nitrogen atoms in azacirculenes, sulfur atoms in thiacirculenes or selenium atoms in selenacirculenes).

Combinations of six- and five-membered rings typical of fullerenes and nanotubes are also encountered in usual highly symmetric organic compounds, which have a closed cyclic structure and include also oxygen- or sulfur-containing rings. Examples of such compounds are tetraoxa[8]circulenes[20] (TOC) **7** and **8**, octathia[8]circulene[21] (OTC) **9** and their selena[22] and aza derivatives[23,24] **10**–**12** — highly symmetric molecules with the unusual inner skeleton, *viz.*, the planar eight-membered carbon ring. Tetraoxa[8]circulenes **7** and **8** were synthesized half a century ago,[20] and their planar structure was established shortly thereafter by X-ray diffraction.[25–27] Octathia[8]circulene was synthesized much later (in 2006).[21] This was an important event in synthetic organic chemistry. In fact, octathia[8]circulene, also referred to as sulflower (a portmanteau of sulfur and sunflower), is a new form of carbon sulfide C_2S.[21] Besides, TOC and OTC proved to be quite chemically inert and thermally stable, due to which their semiconducting properties can be employed for the design of organic field-effect transistors[22,28–31] and light-emitting diodes.[32]

In organic chemistry, not so many highly symmetric cyclic hydrocarbons are known (benzene, coronene, corannulene, fullerenes). All these molecules have high-order symmetry axes and possess, to certain extent, unique physical and chemical properties studied in detail by both experimental and theoretical methods.[11–19] The theory of electronic properties of tetraoxa[8]circulenes, sulflowers and other hetero[8]circulenes has not been considered in detail and not generalized until recently, despite abundant experimental data on the physics and chemistry of these organic compounds. The present review covers the latest advances in investigations of structural, aromatic and spectroscopic properties of hetero[8]circulenes and possible applications of these compounds in semiconductor nanoelectronic devices.

II. X-Ray molecular structures of hetero[8]circulenes

II.1. Hydrocarbon benzocirculenes

Wynberg and Dopper[33] proposed a simple model for explaining the structures and shape of circulene molecules (both hydrocarbon and heterocyclic). According to this model, the shape of the circulene molecule is determined by the sum of the sector angles (Σ_{sect}) of individual rings comprising the macrocycle. According to the X-ray diffraction data,[33,34] the sector of the benzene ring is 60°, whereas the sectors of the five-membered heterocycles are substantially smaller and are equal to 45°, 32° and 35° for thiophene, furan and pyrrole, respectively (Fig. 1). However, in the study by Chernichenko *et al.*,[35] the sector angle of furan was taken equal to 30°. In this approximation,

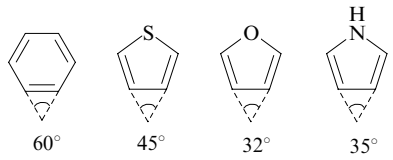


Figure 1. Sector angles for benzene and some heterocycles.[35]

Wynberg–Dopper's structural model is geometrically rigorous. In accordance with this model, coronene is the only planar representative of hydrocarbon circulenes. For this compound, the sum of the sector angles is 360° ($\Sigma_{sect} = 60° \times 6 = 360°$), which corresponds to an unstrained structure of the macrocycle. The X-ray diffraction data support the planar structure of coronene molecules **2**.[36]

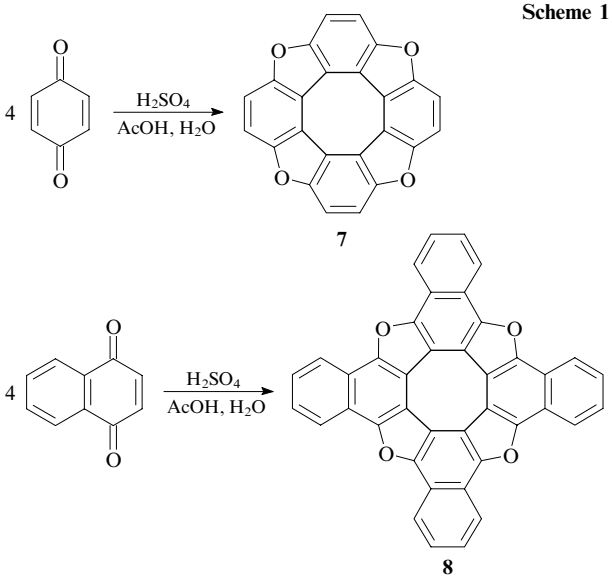
If the sum of the sector angles of circulene is smaller than 360° ('sector deficit'), the macrocycle adopts a truncated cone shape. This shape was revealed by X-ray diffraction for quadrannulene **4** (Refs 8 and 37) and corannulene **1** (Ref. 38). For these compounds, the sums of the sector angles are 240° and 300°, respectively. If the sum of the sector angles of circulene is larger than 360° ('sector excess'), the macrocycle adopts a corrugated (saddle-shaped) structure. This structure was established by X-ray diffraction for [7]circulene[7,39] ($\Sigma_{sect} = 60° \times 7 = 420°$) and the recently synthesized [8]circulene ($\Sigma_{sect} = 60° \times 8 = 480°$). This fact provides excellent support for the quantum chemical predictions of the saddle-shaped structure of [8]circulene published earlier[40–43] and it is in complete agreement with Wynberg–Dopper's structural model.[33] Evidently, the larger the sector deficit or the sector excess, the higher the strain of the macrocycle, resulting in destabilization of the molecule. This is why higher representatives of hydrocarbon circulenes were not isolated in the individual state and are studied by theoretical methods.[40–43] Thus, it was shown[43] that an increase in the size of the macrocycle of benzo[*n*]circulenes ($n = 9–20$) causes the helical twisting of their molecules, *i.e.*, the saddle-shaped conformation is gradually transformed into the helical topology of the molecular skeleton of benzocirculenes.

II.2. Heterocyclic circulenes

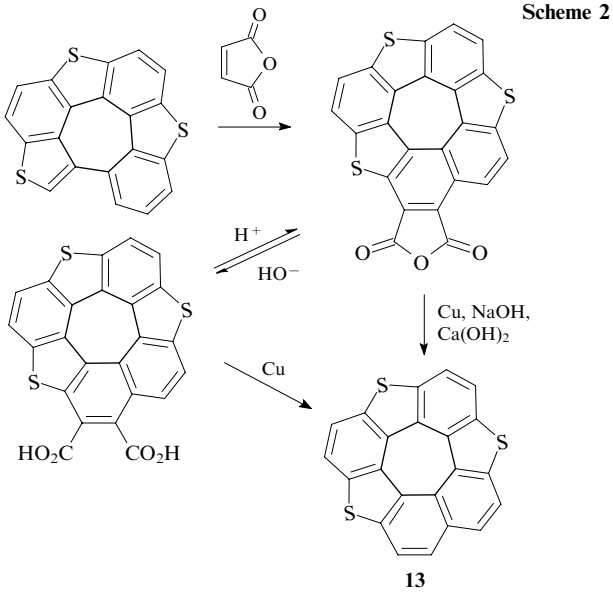
The introduction of five-membered heterocycles into circulenes can substantially extend the range of stable circulene molecules. First heterocirculene **8** of the tetraoxa[8]circulene class was synthesized by Erdtman and Högberg[20] in 1968 by the cyclooligomerization of 1,4-naphthoquinone in the presence of strong mineral acids.[44–48] The simplest TOC **7** was prepared from the starting *p*-benzoquinone in 1970 in a similar fashion (Scheme 1).[44] Somewhat later, Wynberg and Dopper[1] reported the synthesis of the first thiacirculene **13** from the corresponding hexahelicene using an original procedure through the intermediate formation of dehydrohelicene (Scheme 2).[1,49]

Molecules **7** and **8** are unstrained and perfectly planar, as evidenced by X-ray diffraction data.[25–27] This is in complete agreement with Wynberg–Dopper's model ($\Sigma_{sect} = 30° \times 4 + 60° \times 4 = 360°$). The X-ray diffraction data for thiacirculene **13** are absent in the literature; however, a weakly corrugated structure ($\Sigma_{sect} = 45° \times 3 + 60° \times 4 = 375°$) was predicted[33] for this compound based on Wynberg–Dopper's model. Our quantum chemical calculations confirm this conclusion.

Scheme 1



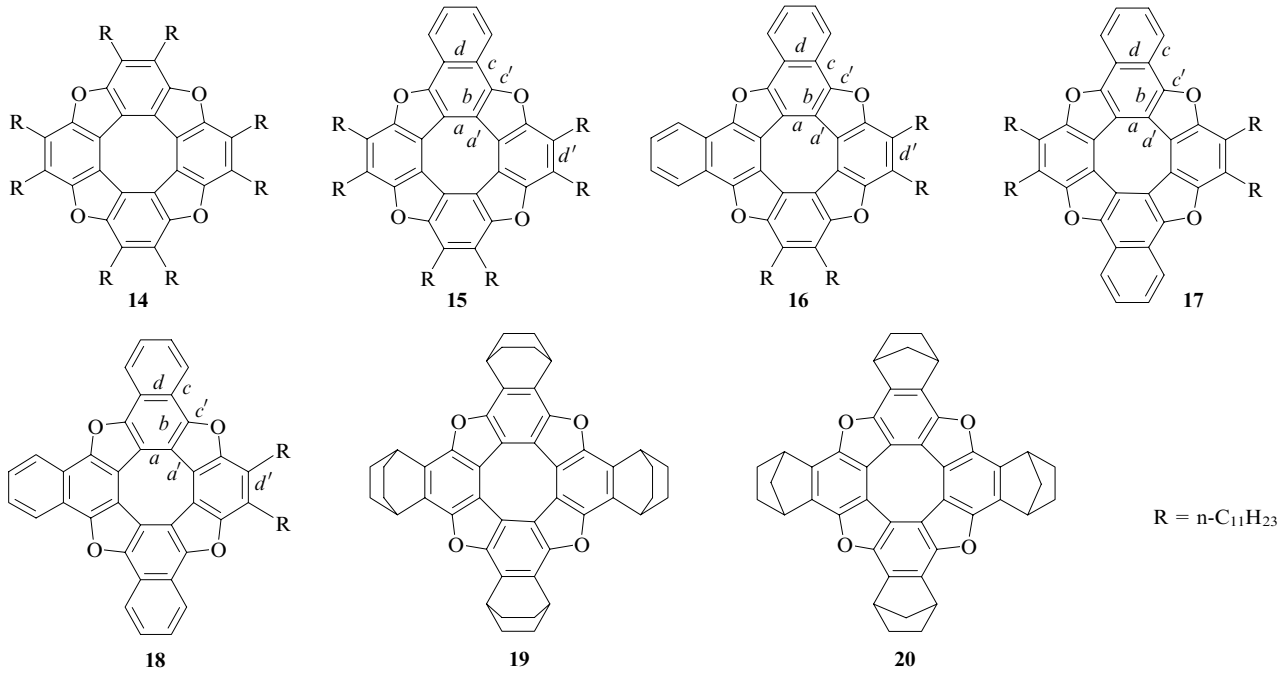
Scheme 2



A new breakthrough in the synthesis of tetraoxa[8]circulenes and thiacirculenes was achieved by research teams headed by Christensen (Denmark)[32,50] and Nenajdenko (Russia).[21,22] A considerable drawback of TOC is their poor solubility in polar and nonpolar solvents, due to which researchers encountered serious difficulties in purifying, identifying and studying spectroscopic properties of these compounds. To eliminate this drawback, Christensen and co-workers[32,50] improved the procedure for the synthesis initially proposed by Erdtman and Högberg (see Scheme 1)[20,44–48] and were the first to synthesize undecyl-substituted TOC **14**–**18** readily soluble in dichloromethane and ethanol.

Independently of Christensen, Rathore and Abdelwahed[51] synthesized bicycloalkyl derivatives of TOC **19**

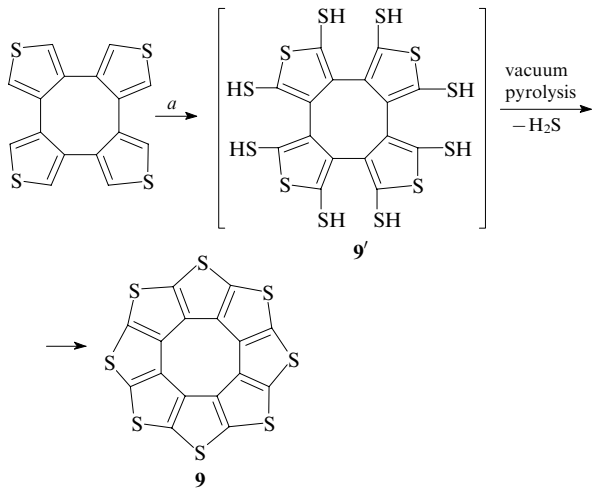
Structures 14–20



and **20** soluble in dichloromethane and benzene. These derivatives form stable radical-cation salts upon the electrochemical oxidation. Wynberg–Dopper's model predicts a planar structure for macrocyclic TOC **14**–**20** ($\Sigma_{sect} = 360^\circ$) because each circulene is based on the parent structure of TOC **7**.

In 2006 the Russian research team headed by V Nenajdenko synthesized the first fully heterocyclic circulene — octathia[8]circulene (sulflower) **9** — by the vacuum pyrolysis of the corresponding cyclic polythiol **9′** (Scheme 3).[21]

Scheme 3



(*a*) 1) Pr^i_2NLi, S, room temperature, 24 h; 2) HCl (aq)

Wynberg–Dopper's model predicts a planar structure of sulflower **9** ($\Sigma_{sect} = 45^\circ \times 8 = 360^\circ$), which was confirmed by X-ray diffraction data.[21, 52, 53] *sym*-Tetraselenatetrathia[8]circulene **10** prepared two years later has a similar planar structure.[22, 28]

Azaoxa[8]circulenes[23, 24] prepared by the group of Pittelkow are the latest synthesized heterocirculenes. Among these compounds are azatrioxa[8]circulene[23] **11**, its dibenzo derivative comprising two naphthalene moieties[23] and diazadioxacirculene[24] **12**. Assuming that the sector angles of the furan and pyrrole molecules are almost equal ($\sim 30^\circ$), Wynberg–Dopper's model predicts a planar structure for azacirculenes. According to the X-ray diffraction data,[23, 24] azacirculene molecules are also planar (apart from alkyl groups) with slight deviations from the planarity for circulene molecules **11** due to strong intermolecular π-stacking interactions in the crystal between two adjacent parallel planes of the macrocycles.

Therefore, the application of Wynberg–Dopper's model to circulenes **1**–**20** gives qualitatively valid conclusions about the strain and shape of the macrocycles. More detailed data on the structures of heterocirculenes, including the geometric parameters of the molecules and the characteristic features of the molecular architecture of the single crystals, can be obtained by X-ray diffraction. The present review focuses on the interpretation of the structures of hetero[8]circulenes and their spectroscopic characteristics.

Table 1 summarizes data on the molecular structures of hydrocarbon and heterocyclic circulenes determined by X-ray diffraction, the bond lengths being averaged taking into account the number of equivalent bonds depending on the symmetry of the molecule. As can be seen in Table 1, the average lengths of the bonds *a* and *c* in the inner and outer rings of hydrocarbon circulenes **1**–**4** vary in narrow ranges of 1.413–1.457 and 1.414–1.440 Å, respectively. The exception is a substantial elongation of the bond *c* in quadrannulene **4** due to the strained macrocycle. A slight alternation of the bonds *a*, *a′* and *c*, *c′* is observed in the inner and outer rings of saddle-shaped benzo[8]circulenes **5**, **6** and hetero[8]circulenes **7**, **8**, **10**–**12**. The average deviations ($\Delta\bar{R}$) between the bond lengths *a*, *a′* and *c*, *c′* for the

Table 1. Bond lengths in circulenes **1–13** determined by X-ray diffraction.

Circulene	$\Sigma_{sect} - 360$ /deg	$a\,(a')$ /Å	b /Å	$c\,(c')$ /Å	$d\,(d')$ /Å	Structure type	Ref.
1	−60	1.413	1.391	1.440	1.403	truncated cone	38
2	0	1.425	1.433	1.415	1.346	planar	36
3	60	1.457	1.434	1.414	1.338	saddle-shaped	7
4	−120	1.450	1.359	1.496	1.396	truncated cone	37
5	120	1.442	1.417	1.432	1.357	saddle-shaped	9
		(1.470)		(1.417)	(1.349)		
6	120	1.434	1.413	1.462	1.404	"	10
		(1.482)	1.462	(1.414)	(1.358)		
7	0	1.406	1.390	1.394	1.377	planar	26
		(1.421)		(1.390)			
8	0	1.414	1.374	1.421	1.439	"	27
		(1.430)		(1.391)			
9	0	1.419	1.380	1.751		"	21
10	0	1.436	1.373	1.793		"	22
		(1.433)	1.793		(1.854)	"	22
11	0	1.403	1.406	1.405	1.398	"	23
		(1.426)		(1.393)			
12	0	1.407	1.402	1.402	1.396	"	24
		(1.428)		(1.390)			
13	15	—	—	—	—	saddle-shaped	33

molecules of these heterocirculenes calculated by Eqn (1) are 0.016 and 0.024 Å, respectively:

$$\Delta\overline{R} = \frac{{}_{n}|l - l'|}{n} \quad (1)$$

where n is the number of circulenes in the set ($n = 5$), l and l' are the corresponding adjacent bond lengths. For benzo[8]-circulenes **5** and **6**, the alternation parameter $\Delta\overline{R}$ is 0.028 and 0.048 Å, respectively. Therefore, the characteristic feature of hetero[8]circulenes is the presence of the planar cyclooctatetraene ring (COTR) with a slight alternation, as opposed to the hypothetically planar COTR with the point-group symmetry D_{4h} characterized by the strict alternation of single (1.472 Å) and double (1.351 Å) bonds.[54–56]

The length of the radial bonds b in benzocirculenes **1–5** gradually increases in the order from the molecules with a angular deficit to the planar unstrained structure of coronene in the series **4** > **1** > **2**, reaches the maximum in [7]circulene **3** and then slightly decreases in structures **5** and **6** with an angular excess. In planar hetero[8]circulenes, the radial bond lengths vary in a narrow range of 1.373–1.406 Å and depend on the nature of the heteroatom. The peripheral bond lengths d in hydrocarbon circulenes decrease from 1.403 to 1.338 Å in a series of circulenes **1** > **2** > **3** with an increase in the angular excess. In higher hydrocarbon [n]circulenes ($n = 8–20$), starting with [8]circulenes **5**, the macrocycle is substantially deformed and twisted,[43] resulting in that the length of the bonds d slightly varies and takes values close to 1.36 Å. In hetero[8]circulenes **7**, **8**, **11** and **12**, the bond d is somewhat longer and its length varies in a range of 1.377–1.398 Å depending on the nature of the heteroatom, except for TOC **8**, in which the bond d is elongated due to the fusion with the benzene ring.

In conclusion it should be noted that all heterocirculenes **7–12** contain a planar eight-membered ring, tetraoxa[8]circulenes **7**, **8** and their N-substituted aza analogues **11**, **12** (AOC) being characterized by slight bond length alternation in the inner COTR in a range of 1.41–1.43 Å. All hydrocarbon circulenes, except for coronene **2** consisting only of benzene rings, are characterized by strong out-of-plane deformation.

III. Crystal structures of hetero[8]circulenes

The planar molecular structure of heterocirculenes **7–10** is responsible for the characteristic features of their single-crystal structures (Fig. 2). Thus, the crystals of tetraoxa[8]-circulene **8** are monoclinic (space group $P2_1/n$) and are composed of closely spaced continuous molecular columns linked by a network of CH···O contacts.[27] Each column consists of planar molecules arranged in a parallel manner; the distance between the nearest planes is 3.38(2) Å. In each pair of adjacent molecules, there are numerous C···C contacts with distances of < 3.5 Å [the shortest distance is 3.41(3) Å] and several C···O contacts (3.41 Å).[27] The molecular crystals of the simplest tetraoxa[8]circulene **7** have a similar structure.[26] The only difference between these two crystal structures is that the shortest interatomic distances between adjacent molecules within the columns of TOC **8** correspond to $C^{\alpha}\cdots C^{\alpha}$ contacts, whereas the shortest interatomic distances between molecules TOC **7** are observed for $C^{\alpha}\cdots C^{\beta}$ contacts (between the furan rings). This indicates that adjacent molecules are shifted to a different extent. All other parameters of the crystal structures of TOC **7** and **8** are very similar.

The crystals of thiacirculenes **9** and **10** have a layered structure (see Fig. 2 *b*) like the crystals of TOC **7** and **8** (see Fig. 2 *a*). According to the X-ray diffraction data, the distance between adjacent parallel molecules in the columns of sulflower **9** is ~ 3.5 Å.[21] The molecules in adjacent columns are tilted with respect to each other by 131°. The S···S distance between adjacent molecules is as short as 3.25 Å, which is comparable with the distance between two sulfur atoms in one molecule (3.23 Å). The electrostatic repulsion between the sulfur atoms in adjacent columns

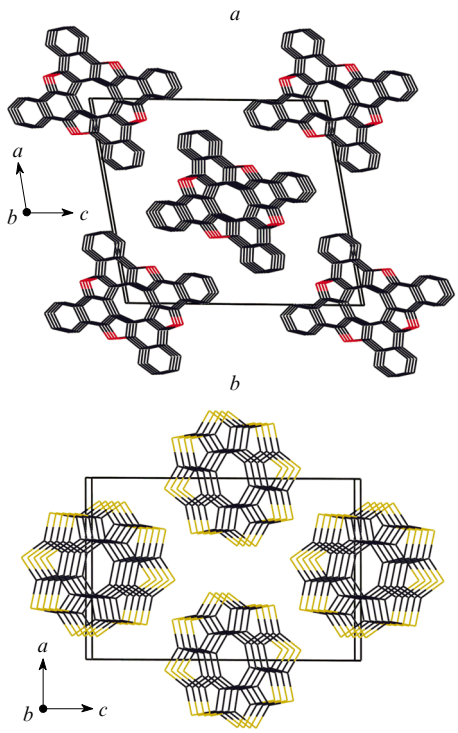


Figure 2. Crystal packing modes of TOC **8** (*a*)[27] and sulflower **9** (*b*).[21]

decreases due to the specific mutual orientation of the molecules. Thus, the sulfur atom of one molecule is located between two sulfur atoms of the adjacent molecule, *i.e.*, three nearest sulfur atoms form an almost regular triangle. Each pair of parallel molecules is stabilized by intermolecular C···C and C···S interactions; the distances between the interacting atoms are 3.5–3.6 and 3.5–3.7 Å, respectively.[52,57] Therefore, the molecular crystals of octathia[8]circulene are stabilized by numerous intermolecular contacts responsible for low solubility of sulflower in organic solvents and high thermal stability (the compound sublimes in the temperature range of 450–530 °C with no signs of decomposition[21]). The crystal packing of *sym*-tetraselenatetrathia[8]circulene **10** (STC) is distinguished by larger intermolecular distances (3.6 Å between parallel molecules in the columns and 3.2–3.3 Å between the nearest molecules in adjacent columns[28]) compared to octathia[8]circulene **9**.

It is interesting that the vacuum sublimation of OTC affords two phases of white and red colour.[52] The white film corresponds to the amorphous state of OTC with the chaotic arrangement of the molecules, whereas the red film consists of single-crystalline OTC having the strictly ordered crystal structure. Evidently, different colours of these phases are associated with the different structural organization of amorphous and crystalline sulflower. Thus, the presence of strong intermolecular interactions in the crystal packing of OTC is responsible for the appearance of an intense colour, whereas the disordered amorphous phase is white. However, the amorphous and crystalline forms of STC have the same white colour.[57] It is hypothesized that intermolecular interactions in single crystals of STC are insufficiently strong to cause perturbations of electron shells of adjacent molecules and the splitting of the energy levels necessary for the colour to appear. This conclusion is in qualitative agreement with the results of calculations of the intermolecular interaction

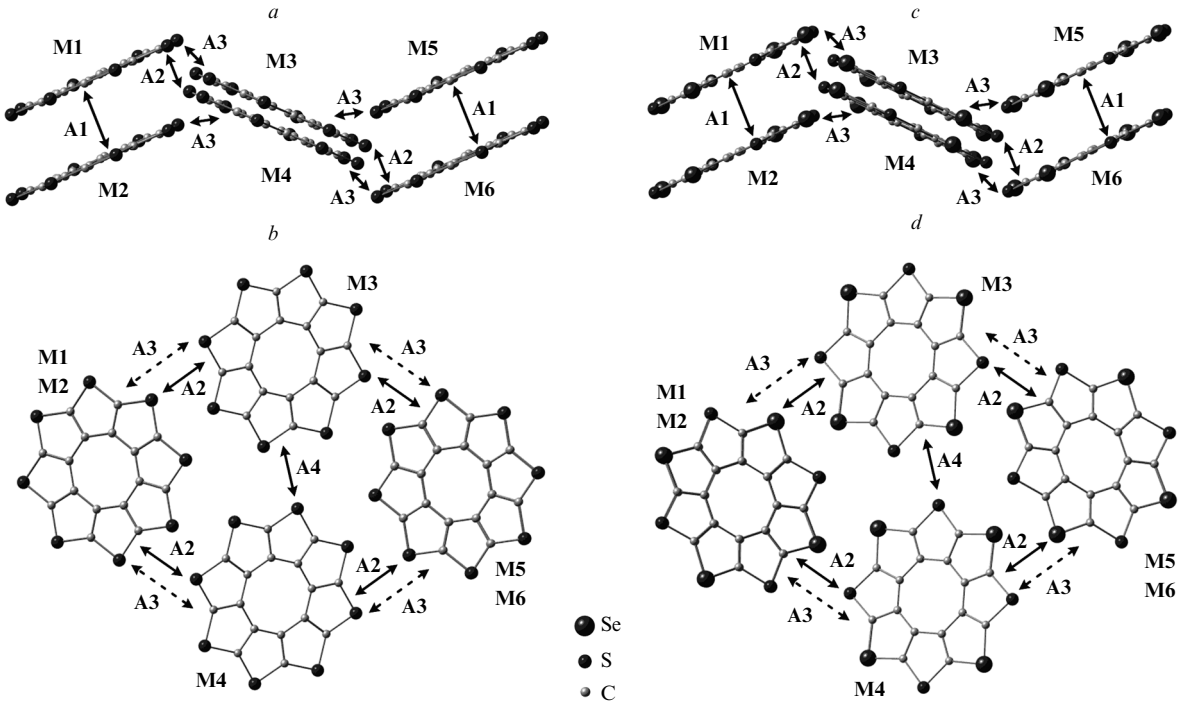


Figure 3. Crystal packing modes of octathia[8]circulene **9** (*a*, *b*) and *sym*-tetraselenatetrathia[8]circulene **10** (*c*, *d*).[57]
The side view (*a*, *c*) and the top view (*b*, *d*). Six molecules are numbered from **M1** to **M6**; the corresponding dimers are from **A1** to **A4**.

Table 2. Total energy of intermolecular interactions in dimers of octathia[8]circulene **9** and *sym*-tetraselenatetrathia[8]circulene **10**.[57]

Circulene	Energy /kcal mol^{-1}				
	A1	**A2**	**A3**	**A4**	hexamer [a]
9	−12.3	−3.0	−4.4	−2.6	−56.8
	(−22.5) [b]	(−2.2) [b]	(−2.1) [b]	(−1.4) [b]	
10	−9.7	−4.0	−2.9	−2.7	−49.7

[a] The stabilization energy of the hexamer was estimated by the formula 2 **A1** + 4 **A2** + 4 **A3** + **A4**.
[b] The values in parentheses were taken from Ref. 61.

energy [57] for the crystal packing modes of OTC and STC taking into account six molecules (Fig. 3). An analysis of the electron density distribution function $\rho(\mathbf{r})$ in terms of Bader's method [58] (Atoms in Molecules, quantum theory, QTAIM analysis) using an additive scheme based on the partitioning of the crystal packing into dimers [57] and the subsequent application of Espinosa's correlation dependence [59, 60] for calculations of the intermolecular interaction energy provided an estimate of the crystal packing energy of OTC and STC at −56.8 and −49.7 kcal mol^{-1}, respectively [57] (Table 2). The π-stacked dimers **A1** make the greatest contribution to the crystal packing energy (see Fig. 3). The total stabilization energy is −12.3 and −9.7 kcal mol^{-1} for OTC and STC, respectively (see Table 2). However, the stabilization energy of the dimer **A1** of OTC estimated [61] at the M06-2x/6-31 + G(d,p) level of theory is −22.5 kcal mol^{-1}, which is almost twice higher compared to the results of our calculations.[57] It is difficult to explain this difference in the energy estimates because the algorithm of calculations employed in the study [61] was not described in detail. In particular, it is unknown whether the correction for basis set superposition errors and the zero-point energy correction were applied. Moreover, the energy of π-stacking interactions estimated in terms of the density functional theory (DFT) strongly depends on the extent to which the non-local Hartree–Fock orbital exchange [62] is taken into account since the contribution of the latter to the M06-2x functional is rather high (54%).[63] Therefore, the stabilization energy of the dimer **A1** of OTC calculated in the study [61] is apparently substantially overestimated because of the overestimation of the orbital exchange.

The intermolecular S···S and S···Se interactions in the dimers **A2**–**A4** (see Fig. 3 *a*,*c*) are rather weak; however, taking into account the number of equivalent dimers in the hexamer, they provide strong binding of adjacent molecular columns and are to a large extent responsible for high stability of the crystals of OTC and STC.

Besides, the characteristic distinguishing feature of circulenes **9** and **10** is the morphology of in-vacuum prepared films. According to the results of atomic force microscopy,[22] the surface area and the height of the crystal nuclei of octathia[8]circulene **9** are 12 000 nm^2 and 10–12 nm, respectively, after the film growth for 1 min, whereas the crystal nuclei of circulene **10** reach substantially smaller sizes (the surface area is 1200 nm^2 and the height is 2–5 nm) during the same period of time. The grains of sulflower **9** continue to grow with time and fill the surface of the support, after which the growth occurs in the direction perpendicular to the surface of the substrate. Due to a much smaller size, the grains of circulene **10** fill the total surface of the substrate at once with no signs of the lateral growth to form a high-dispersion film compared with circulene **9**.

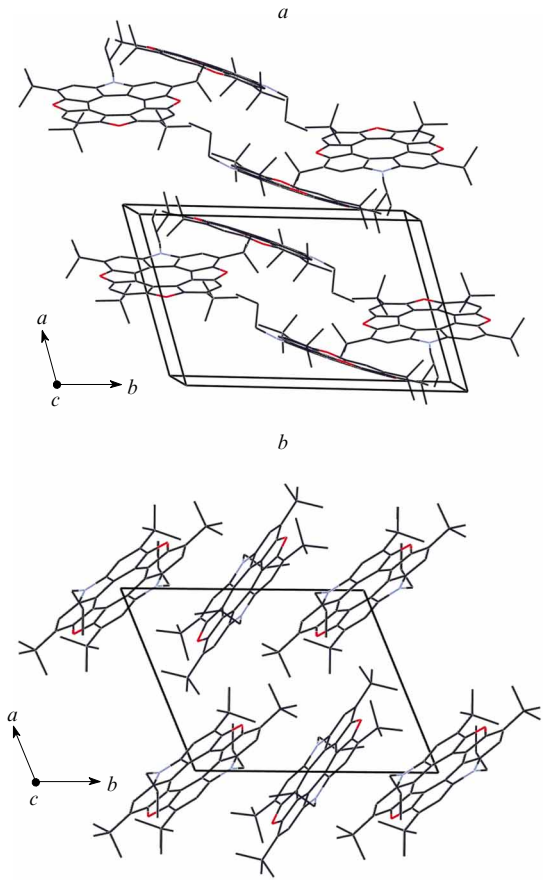


Figure 4. Crystal packing modes of azaoxa[8]circulenes **11** (*a*) [23] and **12** (*b*).[24]

The functionalization of hetero[8]circulenes leads to changes in the structural organization of the crystals. In particular, the introduction of alkyl substituents into the outer perimeter of circulenes hinders stacking interactions between the molecules in the crystal.[23, 24, 64] Thus, in the condensed state tetra-*tert*-butyl-substituted azatrioxa[8]circulene **11** (Fig. 4 *a*) is associated to form isolated π-stacked dimers (the distance between the parallel planes of the molecules is 3.4 Å), resulting in a slight deformation of the macrocycle and a sligh deviation from the planarity of COTR to form a truncated cone-shaped structure. The presence of four *tert*-butyl and two n-propyl substituents in the outer perimeter of diazadioxa[8]circulene **12** interferes with the formation of π-stacked dimers in the crystalline phase (see Fig. 4 *b*): the molecules form infinite zigzag ribbons in the *ac* plane rotated with respect to each other by 45°. A similar zigzag arrangement of molecules in the crystal and the absence of aggregation (the tilt angle of the ribbons is ~70°) is observed also in tetra-*tert*-butyltetraoxa[8]circulene (Bu^t_4-TOC) **21** characterized by the regular arrangement of the substituents along the outer perimeter (Fig. 5 *a*).[64, 65]

Interesting data on the observed aggregation of Bu^t_4-TOC in solution and the crystalline phase have been reported.[64]

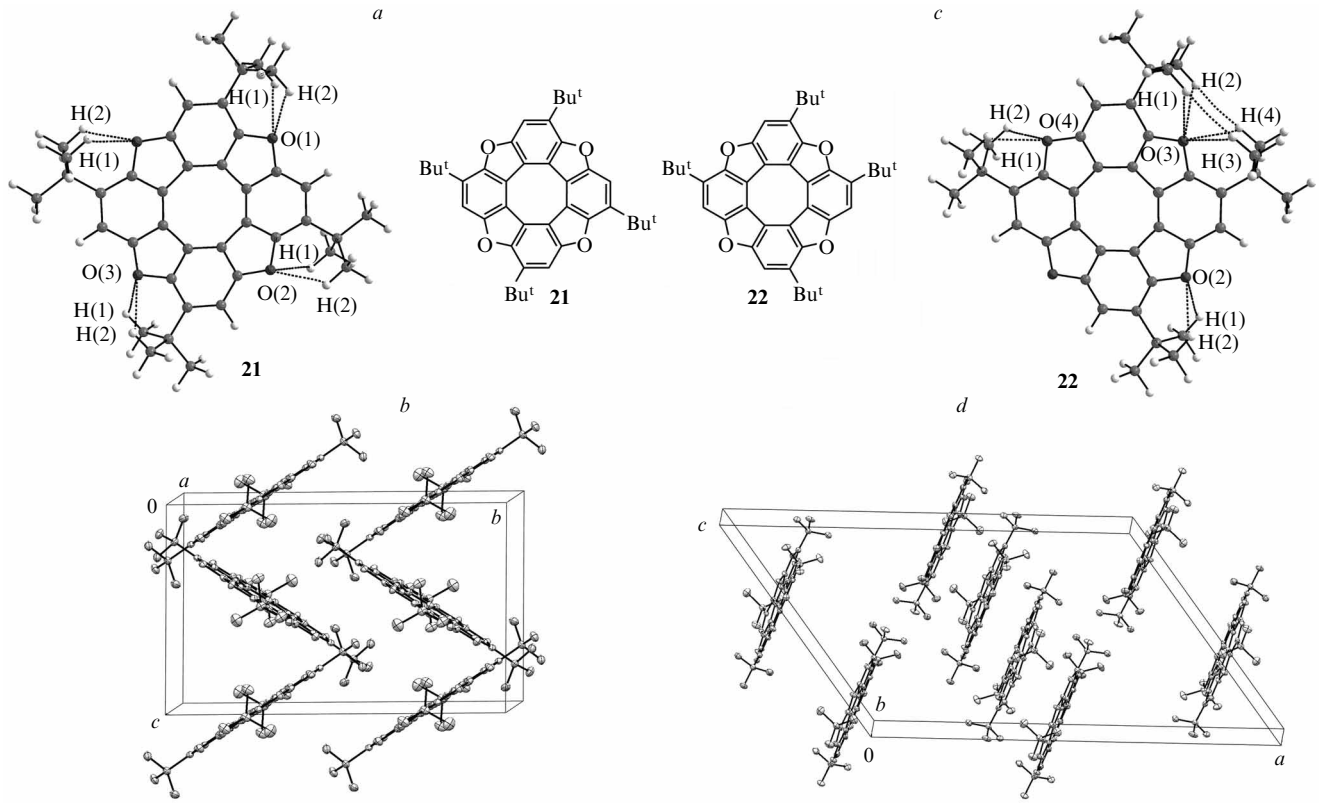


Figure 5. Equilibrium structures of two regioisomers (**21** and **22**) of tetra-*tert*-butyltetraoxa[8]circulene (*a*, *c*) and their crystal packing modes (*b*, *d*) (intramolecular hydrogen bonds determined by the QTAIM method are indicated by dashed lines).[65]

In this case, the fact of aggregation is rather strange taking into account the presence of four bulky *tert*-butyl substituents in the outer perimeter, which usually hinder the aggregation of organic molecules.[66–68] The unusual behaviour of this circulene in solution was explained[64] based on the mechanism of cooperative polymerization.[69] Besides, it was shown[65] that the aggregation of Bu^t_4-TOC can also occur by a key–lock mechanism involving the aggregation and, in particular, dimerization of the molecules in such a manner that a molecule of one of the four possible regioisomers[65] provides a free space for the location of *tert*-butyl groups of a molecule of another regioisomer. In this situation, one molecule acts as a lock that accepts a specific key molecule. This mechanism is supported by the X-ray diffraction data for two regioisomers of Bu^t_4-TOC **21** and **22** (see Fig. 5), which differ in the arrangement of *tert*-butyl substituents. Thus, regioisomer **21**, in which the Bu^t groups are arranged in a regular manner, does not form π-stacked dimers in the crystalline phase, as shown above. However, π-stacked dimers were found in the crystal packing of regioisomer **22** (see Fig. 5 *b*) characterized by a large free volume in the outer perimeter due to the irregular arrangement of the substituents. Therefore, the aggregation of regioisomers of Bu^t_4-TOC in solution is possible only in the presence of several regioisomeric forms, and the quantitative distribution over the conformers is to a large extent determined by the positions of the *tert*-butyl groups and stabilization effects through intramolecular CH···O hydrogen bonds (see Fig. 5).[65]

IV. Quantum chemical studies of the structures of hetero[8]circulenes

IV.1. Hypothetical heterocirculenes

Modern quantum organic chemistry is being actively developed due to a great progress in computational technologies, the design of various software for quantum chemical simulation accessible to a broad range of users and the improvement of quantum chemical approximations. As a result, quantum chemistry currently provides qualitatively new predictions because it can be used to simulate the structure and properties of new molecules and materials in early steps of their design.

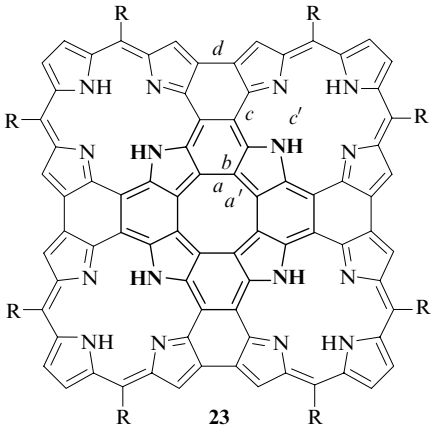
For instance, [8]circulene **5′**, which was synthesized as late as in 2013,[9] was studied in detail by quantum chemical methods at different levels of theory[40–42] 10 years prior to its successful synthesis, and the calculated shape and structural parameters proved to be consistent with the X-ray diffraction data[9] (circulene **5′** is a simpler analogue of compounds **5** containing no methyl and aryl substituents, the cyclic structure of which was correctly predicted to have a saddle-shaped form with D_{2d} symmetry).[40–42] The structure and some energy properties of quadrannulene **4** were also predicted[43] shortly before the first synthesis[8] of this bowl-shaped representative of benzocirculenes in 2010. Therefore, the specific features of the electronic structures of hypothetical heterocirculenes or those which were not isolated in the individual state deserve special consideration in the present review.

Nakamura *et al.*[70] synthesized planar tetramer **23** of the free-base porphyrin and the corresponding tetrame-

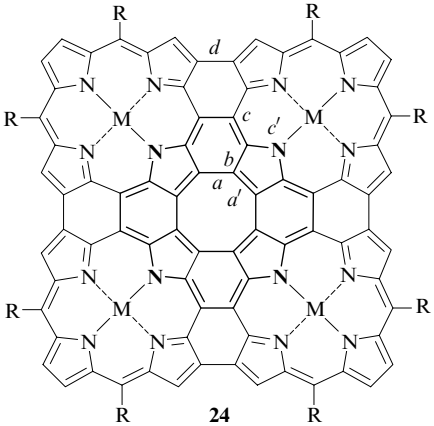
talloporphyrins **24** (see Refs. 70–72) based on planar tetraaza[8]circulene. The structural parameters of tetramers **23** and **24** were studied [70–72] in terms of the density functional theory [73, 74] using the B3LYP exchange correlation functional [75, 76] and the 6-31G(d) [77] (for N, C and H atoms) and Lanl2DZ [78] (for Zn atoms) basis sets. (The structural data are presented in Table 3 at the end of Section IV.) It was shown that the alternation of the bond lengths a and a' (ΔR) in the inner COTR is rather small (0.039 and 0.052 Å for tetramers **23** and **24**, respectively, where M = Zn); however this alternation is substantially larger than that observed for TOC **7** and **8** (ΔR = 0.015 and 0.016 Å, respectively) and azaoxa[8]circulenes **11** and **12** (ΔR = 0.023 and 0.021 Å, respectively). For comparison, the parameter ΔR for free cyclooctatetraene with D_{2d} symmetry and hypothetical planar COTR with D_{4h} symmetry is substantially larger (0.133 and 0.121 Å, respectively).[54, 79] Therefore, the characteristic equalization of the C–C bond lengths is observed in the inner ring of hetero[8]circulene molecules, which is inherent in most of aromatic molecules.[80] However, quantum chemical calculations in terms of the theory of nucleus-independent chemical shifts (NICS) [80, 81] for circulenes **9**–**12**, **14**–**20**, **23** and **24** disprove the aromatic character of COTR and predict its antiaromaticity.[23, 24, 70–72, 82, 83] (In the case under consideration, the terms 'aromaticity' and 'antiaromaticity' imply the prevalence of diatropic/paratropic ring currents in the cyclic conjugated system, which is the necessary characteristic feature of aromatic/antiaromatic systems.)

The structural and aromatic properties of hypothetical heterocirculenes **25** and **26** were recently studied by Gribanova *et al.*[84, 85] by the DFT/B3LYP/6-311G(d) method.[73–76, 86] In particular, it was shown that the shape of the macrocycle of these heterocirculenes is governed by the balance between the steric factor and the effect of the π-electron delocalization depending on the electronegativity of the heteroatoms X and Y. An increase in the size of peripheral Y atoms and the expansion of the inner ring lead to a gradual change from the bowl-shaped structure of circulenes (Y = N, BF_2) to the planar and then to the saddle-shaped structure (Y = P, As, AlF_2, GaF_2), which is in good agreement with Wynberg–Dopper's structural model.[33] In addition, it was shown [84, 85] that [8]circulenes **25b** (n = 4, X = N, Y = BF_2) and **25c** (n = 4; X = Y = BF_2) can undergo stacking dimerization to form hypothetical heterofullerenes, for which high stability and proton affinity were predicted. An idea of the design of functional heterofullerenes based on heterocirculenes has also been proposed.[87] In particular, it was shown that the fullerene $C_{32}N_{16}$ constructed by the stacking dimerization of heterocirculene **27** (N-containing analogue of sulflower **9**) is thermodynamically stable and is highly prone to hydrogenation.

Structures 23–31

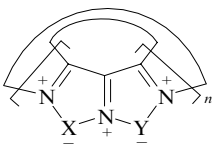


23



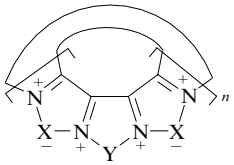
24

M = Zn, Cu; R = 3,5-$Bu^t_2C_6H_3$



25

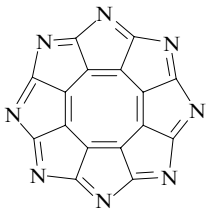
n = 4, 5



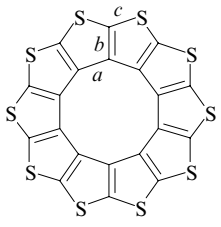
26a–c

n = 3

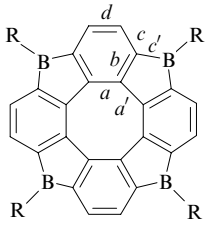
X = Y = N, P, As (**a**); X = N: Y = BF_2, AlF_2, GaF_2 (**b**);
X = Y = BF_2, AlF_2, GaF_2 (**c**)



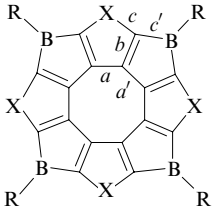
27



28

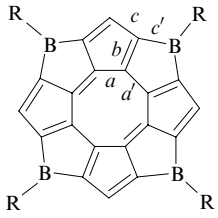


29



30a,b

X = S (**a**), BR (**b**)



31

29–31: R = 4-MeC_6H_4

Table 3. Bond lengths in molecules of selected heterocirculenes estimated by quantum chemical calculations.

Circulene [a]	Approximation	$a\,(a')$/Å	b Å	$c\,(c')$ Å	$d\,(d')$ Å	ΔR [b]	Ref.
7 S_0 (D_{4h})	B3LYP/6-31G(d,p)	1.396 (1.431)	–	–	–	0.035	92
	B3LYP/6-31G(d)	1.396 (1.431)	1.400	1.400 (1.385)	1.403	0.035	96, 97
7 T_1 (C_{2v})	UB3LYP/6-31G(d)	1.424 (1.396)	1.421	1.378 (1.385)	1.437	0.028	96
8 (D_{4h})	B3LYP/6-31G(d)	1.415 (1.429)	1.387	1.424 (1.380)	1.445	0.014	97
9 (D_{8h})	B3LYP/6-31G(d,p)	1.425	1.381	1.766		0	91, 92
	PW-91/TZP	1.420	1.380	1.760		0	93
	B3P86/6-31G(d,p)	1.418	1.378	1.755		0	94
10 (D_{4h})	B3P86/6-31G(d,p)	1.429 (1.431)	1.383	1.738 (1.870)		0.002	94
11 (C_s)	B3LYP/6-31G(d)	1.401 (1.430)	1.412	1.409 (1.397)	1.403	0.029	100
12 (C_s)	B3LYP/6-31G(d)	1.402 (1.436)	1.415	1.402 (1.394)	1.405	0.034	100
15, 16, 18 (C_{2v}), **17** (D_{2h}) (R = H)	B3LYP/6-31G(d)	1.413 (1.430)	1.385	1.425 (1.382)	1.446 (1.403)	0.017	98
23	B3LYP/6-31G(d)	1.401 (1.440)	1.401	1.407 (1.436)	1.408	0.039	71
24 (M = Zn)	B3LYP/6-31G(d)(C, N, H)/ Lanl2DZ (Zn)	1.392 1.444	–	–	–	0.052	70
28 S_0 (C_2)	B3LYP/6-311G(d)	1.479	1.399	1.723		–	88
28 T_1 (C_s)	UB3LYP/6-311G(d)	1.376–1.471	1.386–1.485	1.725–1.769		–	88
29 (C_4)	B3LYP/6-31G(d)	1.403 (1.526)	1.449	1.384 (1.542)	1.393	0.123	89
30a (C_4)	B3LYP/6-31G(d)	1.392 (1.464)	1.398	1.741 (1.588)		0.072	89
30b (C_8)	B3LYP/6-31G(d)	1.434	1.410	1.588		0	89
31 (C_4)	B3LYP/6-31G(d)	1.405 (1.386)	1.458	1.425 (1.579)		0.019	89
COTR (D_{4h})	CASSCF(8,8)/6-31G(d,p)	1.472 (1.351)				0.121	54

[a] S_0 is the singlet ground state, T_1 is the lowest triplet excited state; [b] for the bonds a and a'.

The structure of hypothetical decathia[10]circulene **28** was studied [88] by the B3LYP/6-311G(d) method [73–76, 86] in the ground and electronically excited states. It was shown that circulene **28** has a corrugated shape in the singlet ground electronic state (the point symmetry group C_2). This is in good agreement with Wynberg–Dopper's model ($\Sigma_{sect} = 10^\circ \times 45 = 450^\circ$). The S···S distance between adjacent thiophene rings is 3.03–3.04 Å and this value is shorter than the corresponding distance in circulene **9** (3.23 Å). This is associated with the contraction of the thiophene rings along the lateral edges in circulene **28** due to an expansion of the macrocycle. In the triplet state, the symmetry of the decathia[10]circulene molecule is C_s, and the molecule is strongly deformed, resulting in a large scatter in the bond lengths a and a' in the inner ring (see Table 3 at the end of Section IV). The bonds b, c and c' are also essentially nonequivalent. Evidently, the state T_1 of circulene **28**, which is discussed in Ref. 88, either does not have a pronounced minimum or appears as a local minimum on the potential energy hypersurface for the T_1 state.

The recently studied [89] hypothetical circulenes **29**–**31** containing four boron atoms are of particular interest in view of their electronic structures. In particular, it was shown that the presence of electron-deficient boron atoms has a substantial effect on the π-electron delocalization in the macrocycle. As a consequence, circulenes **30b** and **31** are fully aromatic (the inner COTR and the surrounding rings become aromatic as opposed to all known hetero[8]circulenes), whereas circulenes **29** and **30a** contain, on the contrary, the antiaromatic inner ring surrounded by a nonaromatic system of rings. Actually, the large bond length alternation parameter for the C=C bonds in the inner COTR of compounds **29** and **30a** is indicative of the absence of effective cyclic conjugation responsible for the production of diamagnetic ('aromatic') ring currents. It should be noted that circulenes **29** and **30** have a planar structure characteristic of most of unstrained hetero[8]circulenes, whereas circulene **31**, as well as its structural analogue [8,5]coronene, are bowl-shaped.[90]

IV.2. Synthesized hetero[8]circulenes

Quantum chemical studies of the structures of the synthesized hetero[8]circulenes cover all classes and include, in particular, thia[8]circulenes [91–95] **9** and **10**, tetraoxa[8]circulenes [92, 96–99] **7**, **8** and **15**–**18** (R = H) and azaoxa[8]circulenes [23, 24, 100] **11** and **12** (Table 3). Calculations with full

geometry optimization predict a planar structure of the macrocycle for all the above-mentioned circulenes. In particular, a molecule of TOC **7** in the singlet ground state is planar (point symmetry group D_{4h}). The inner eight-membered ring has a system of short (1.396 Å) and long (1.431 Å) C–C bonds: short bonds belong to the benzene rings; long bonds, to the furan rings. The excitation of TOC **7** to the first triplet excited state is accompanied by distortion of the molecular symmetry (point symmetry group C_{2v}) as a result of the formation of the antiquinoid structure of the benzene rings compared to the pure aromatic structure in the singlet ground state. Besides, there is a different pattern of the single and double bond alternation in the inner COTR. Tetraoxa[8]circulene molecules **15**–**18** (R = H) containing naphthalene moieties have identical structural parameters (the deviations of the bond lengths are not larger than 0.00 Å; the bond angles differ by no more than 1°). The distinguishing feature of these compounds is the small alternation parameter for the inner ring (ΔR = 0.017 Å). The parameter ΔR for tetraoxa[8]circulene **8** containing four naphthalene moieties is even smaller and is equal to 0.014 Å. This is indirect evidence that the inner COTR has a weak antiaromatic character. This conclusion correlates well with the calculations of other aromaticity indices in the series of TOC **7**, **8** and **15**–**18** (R = H).[82,83]

In our studies, we always pay attention to the triplet state T_1, optimize its geometry and endeavour to predict phosphorescence and other properties of the triplet T_1. In terms of the spin-catalysis concept,[12] the triplet state is not only responsible for the photochemical properties of the substance but also greatly influences its catalytic reactions (both in the presence of homogeneous and heterogeneous catalysts). The triplet T_1 may also have an effect on the magnetic properties and NMR spectroscopic parameters of diamagnetic compounds.

A comparison of the structural parameters of aza[8]circulenes **11** and **12** with those of furan, pyrrole and benzene molecules shows that the condensation leads to a more substantial elongation of the C–O and C–N bonds compared with the C=C bonds of the benzene moieties. However, on the whole, there is a tendency to the expansion of benzene, furan and pyrrole rings involved in the macrocycle (compared to the free molecules) and to equalization of C=C, C–O and C–N bond lengths in the outer perimeter. The bond length equalization in the outer perimeter of azaoxa[8]circulenes and tetraoxa[8]circulenes attests to their aromatic character, like the characteristic signals of 'aromatic' protons in the ^{1}H NMR spectra.[23,24] Although being planar, the inner octatetraene ring has the antiaromatic character, as evidenced also by recent calculations[23,24] of nucleus-independent chemical shifts[80,81] in the centre of the octatetraene ring [NICS(0)] and 1 Å above the centre [NICS(1)]. These indices have positive values and attest to the dominant role of antiaromatic paramagnetic ring currents in COTR.

Sulflower molecules **9** and **10** are distinguished among all other hetero[8]circulenes by high symmetry and the absence of hydrogen atoms. According to the results of DFT calculations, octathia[8]circulene **9** has the singlet ground state $^1A_{1g}$ and the point group of symmetry D_{8h}. Therefore, the structural parameters of these compounds include only three bond lengths (see Table 3). Due to high symmetry, the bond length alternation in the inner ring is unavoidably absent, which is in agreement with the X-ray diffraction data. For selenium-containing sulflower **10**, the alternation parameter is negligibly small (0.002 Å); however, this is not evidence of the aromaticity of the compound. Numerous calculations[52,92,94] demonstrated that sulflowers are systems with unusual electronic structures. Thus, the inner ring is strictly antiaromatic, and the surrounding system of thiophene and selenophene rings is aromatic and stabilizes the planar structure of these molecules. The calculation of the ring current strength in molecule **9** by the GIMIC (gauge including magnetically induced current) method[101,102] showed that the total ring current is almost equal to zero (-0.2 nA T^{-1}). This is indicative of the mutual compensation of the paratropic ring current in the inner eight-membered ring and the outer-perimeter diatropic ring current (Fig. 6 *a*). Similar conclusions were drawn for selenasulflower **10** (the total current strength is 0.6 nA T^{-1}) and tetraoxa[8]circulene **7** (Fig. 6 *b*; -2.2 nA T^{-1}), as well as for all other tetraoxa[8]circulenes and azaoxa[8]circulenes, with the difference that weak induced magnetic currents are observed in the selenophene and benzene rings of the latter compounds.

In summary of the structural part of the review, it should be noted that the application of Wynberg–Dopper's structural model[33] to heterocirculene molecules gives qualitatively correct predictions of the shape of these molecules, which are usually in good agreement with the X-ray diffraction data. However, in some cases, the structure of heterocirculenes proved to be sensitive to stacking interactions between molecules in the crystal,[23] which are not taken into account in terms of Wynberg–Dopper's model. In addition, this model is not geometrically rigorous, because the sector angles for most of the rings differ from the ideal values of 30°, 45° or 60° (see Refs 33–35) and vary depending on the efficiency of π-conjugation. As a consequence, some structures which are planar according to the results of X-ray diffraction study and quantum chemical calculations have an angular excess or deficit. For example, assuming that the sectors of furan and pyrrole are 32° and 35°, respectively (rather than 30°, which was used for simplicity in the studies[23,35]), circulene molecules **7** and **12** have a sector excess of 8° and 14°. These values correspond to a quasiplanar saddle-shaped structure and are inconsistent with the X-ray diffraction data. Evidently, in these cases, the effective π-conjugation is essential for the planar structure. This factor is responsible for the specific aromatic

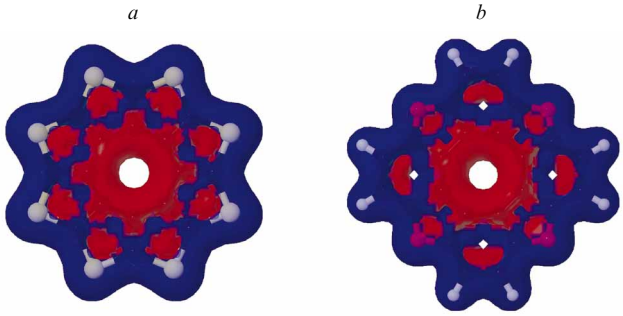


Figure 6. Ring current density in octathia[8]circulene **9** (*a*) and tetraoxa[8]circulene **7** (*b*).[103] The diatropic ring current density is shown in blue; the paratropic ring current density is red.

character of the macrocycle as a whole and stabilizes its planar structure.

V. Spectroscopic properties of hetero[8]circulenes

The optical spectra of hetero[8]circulenes are of particular interest because these compounds are promising materials for organic light-emitting diodes (OLED)[32] and organic field-effect transistors.[22, 29–31, 95, 104, 105] However, researchers encountered serious difficulties in investigating the optical spectra of hetero[8]circulenes because of very low solubility of these compounds in the majority of known solvents. This problem can be eliminated by introducting alkyl substituents (for example, Pr^n, Bu^t, n-$C_{11}H_{23}$) into the outer perimeter of hetero[8]circulenes.[46, 50, 64] Alkyl derivatives of heterocirculenes are readily soluble in organic solvents. This allowed researchers to study their spectroscopic properties by different experimental methods of molecular spectroscopy and mass spectrometry.

V.1. Mass-spectrometric studies

The first mass spectra of heterocirculenes were obtained by Högberg[44–46] for TOC **7** and **8** and their derivatives (electron impact ionization, the electron energy was 70 eV, the temperature in the chamber was 250 °C). The mass spectrum of circulene **8** shows only three characteristic signals at *m*/*z* 560 (M^+, 100%), 280 (M^{2+}, 36%) and 186.7 (M^{3+}, 6%) (Table 4). No other signals with an intensity of >1% were observed in the mass spectrum of TOC **8**. These data attest to exceptionally high stability of the molecular ions M^+, M^{2+} and M^{3+} of TOC **8**, as well as to the π-electronic character of these ions, *i.e.*, unpaired electrons of the radical cations M^+ and M^{3+} and of the excited M^{2+} cation lie in the π-orbitals and are strongly delocalized.

In contrast to TOC **8**, the mass spectrum of tetraoxa[8]circulene **7** obtained under the same conditions is more complicated. It was shown[44] that, apart from unfragmented molecular ions M^+ and M^{2+}, the mass spectrum contains ions that are formed as a result of efficient dissociation of M^+ and M^{2+} with the successive elimination of four CO fragments (M_r = 28) (see Table 4). In our opinion, the unidentified peaks at *m*/*z* 152 and 120 belong to the $[M-2\,CO]^{2+}$ and M^{3+} ions, respectively. The mass spectra of alkyl-substituted TOC **14** (R = Me, Pr^n)[46] display, apart from characteristic signals of M^+ and M^{2+} ions, the elimination of alkyl substituents. Thus, peaks corresponding to the successive elimination of six methyl groups from the molecular ion were identified in the mass spectrum of TOC **14** (R = Me).[46] The intensity of these peaks monotonically decreases with an increase in the number of lost methyl groups. In the mass spectrum of propyl-substituted TOC **14**, numerous peaks were identified and assigned to the successive elimination of 19 alkyl carbon atoms from M^+ and M^{2+} ions (see Table 4).

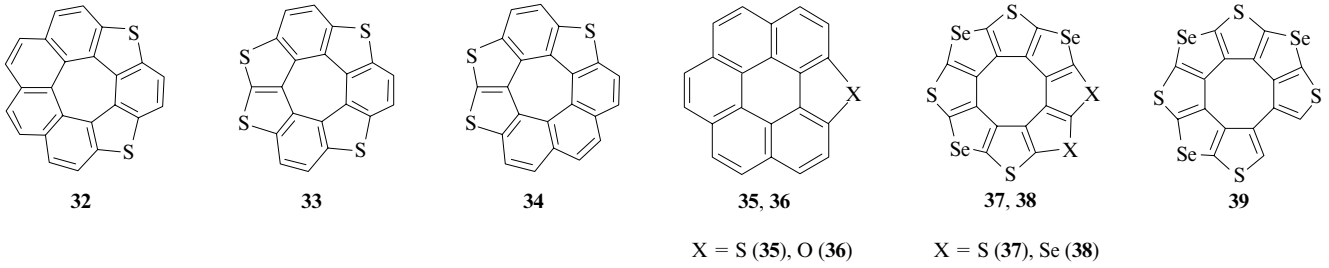
Circulenes **15**–**18** (R = H) belong to mixed TOC because these compounds contain benzene and naphthalene moieties in different ratios. All these compounds give similar mass spectra,[45] which show two main peaks belonging to mono- and dications M^+ and M^{2+}. The experimental data on the fragmentation of M^+ and M^{2+} accompanied by the elimination of CO groups (like for TOC **7**) are absent.

Dopper and Wynberg made an essential contribution to investigations of the mass spectra of heterocirculenes[1, 33] by studying a series of thia[7]circulenes **13** and **32**–**34** with different numbers of tiophene units in different positions. The mass spectra of these circulenes show only peaks

Table 4. Parameters of main peaks in the mass spectra of heterocirculenes.

Circulene	*m*/*z* (assignment, intensity)	Ref.
7	360 (M^+, 100%), 332 ($[M-CO]^+$, 1.2%), 304 ($[M-2\,CO]^+$, 7%), 304 ($[M-3\,CO]^+$, 3.5%), 248 ($[M-4\,CO]^+$, 11%), 180 (M^{2+}, 14%), 152 ($[M-2\,CO]^{2+}$, 4%), 124 ($[M-4\,CO]^{2+}$, 16%), 120 (M^{3+}, 1.2%)	44
8	560 (M^+, 100%), 280 (M^{2+}, 36%), 186.7 (M^{3+}, 6%)	44, 45
9	448 (M^+)	35
10	639.5 (M^+, 81%), 319.8 (M^{2+}, 15%), 685 (**38**$^+$, 2%), 589 (**37**$^+$, 8%), 560 (**39**$^+$, 39.5%), 479.7 ($[M-2\,Se]^+$, 9.4%)	22
11	625 (M^+)	23
13	368 (M^+, 100%), 184 (M^{2+}, 40%)	1, 33
14 (R = Me)	472 (M^+, 100%), 457 ($[M-CH_3]^+$, 14%), 236 (M^{2+}, 17%), 228.5 ($[M-CH_3]^{2+}$, 13%)	46
14 (R = Pr^n)	696 (M^+, 100%), 348 (M^{2+}, 16%); 667 (17%), 639 (5%), 623 (4%), 595 (4%), 333.5 (7%), 319.5 (6.5%), 305 (11%), 291 (25%), 269 (7%)	46
15 (R = H)	410 (M^+), 205 (M^{2+}, 16%)	45
16 (R = H)	460 (M^+, 100%), 230 (M^{2+}, 33%)	45
17 (R = H)	510 (M^+, 100%), 255 (M^{2+}, 57%)	45
15–**18** (R = n-$C_{11}H_{23}$)	**15**: 1335 (M^+); **16**, **17**: 1077 (M^+); **18**: 818.4 (M^+)	32
19, **20**	**19**: 680.8 (M^+); **20**: 624.7 (M^+)	51
21	584.7 (M^+)	64
23, **24**	**23**: 2724.1 (M^+); **24** (M = Zn): 2977.4 (M^+); **24** (M = Cu): 2968.5 (M^+)	70, 71
32	362 (M^+, 100%), 181 (M^{2+}, 35%)	33
33	374 (M^+, 100%), 187 (M^{2+}, 80%)	33
34	368 (M^+, 100%), 184 (M^{2+}, 50%)	33
35	306 (M^+)	33
36	290 (M^+), 145 (M^{2+})	33

Structures 32 – 39



32 **33** **34** **35, 36** **37, 38** **39**

X = S (**35**), O (**36**) X = S (**37**), Se (**38**)

assigned to the molecular ions M^+ and M^{2+}. The further fragmentation of these ions is minor, which attests to their high stability. For example, the intensity of the $[M-S]^+$, $[M-H_2S]^+$, $[M-CHS]^+$, $[M-CH_3S]^+$ and $[M-C_2S_2]^+$ fragment ions is not higher than 4%.[33] The exception is tetrathia[7]circulene **33**. In the mass spectrum of the latter compound, the intensity of the peak of $[M-CHS]^+$ ions is 8%. It should be noted that this is the only ion identified in the mass spectra of all thia[7]circulenes **13** and **32** – **34**.

Thiacoronene **35** is yet another example of the synthesized heterocirculenes. A characteristic feature of this compound is that it is easily oxidized to form the corresponding sulfone. The mass spectrum of the latter shows, apart from a molecular ion peak at *m*/*z* 338, intense peaks at *m*/*z* 290 and 145 assigned to mono- and dications of oxocoronene **36**.[33] The unusually intense peak at *m*/*z* 290 attests to high stability of the molecular ion of oxocoronene **36**.

Up-to-date mass-spectrometric studies of heterocirculenes[23, 24, 32, 51, 70, 71] are usually limited to the identification of the molecular ion M^+ with the goal of establishing the molecular formula of the compound as a supplement to more reliable NMR spectroscopy. In particular, mass spectrometry was used to confirm the qualitative and quantitative compositions of sulflower **9**, azacirculene **11**, TOC **15** – **20** and porphyrin tetramers **23** and **24**.

The mass spectrum of circulene **10** is rather complicated,[22] which is not typical of most of hetero[8]circulenes. In particular, peaks of unsymmetrical circulenes of composition $C_{16}S_5Se_3$ (**37**) and $C_{16}S_3Se_5$ (**38**), as well as of dehydrohelicene $C_{16}H_2S_4Se_3$ (**39**), were identified in this spectrum. These compounds are formed as impurities[35] in the synthesis of the target circulene **10**. Unfortunately, only the molecular ion at *m*/*z* 448 (M^+) was identified in the mass-spectrometric study of sulflower **9**.[35] Therefore, the formation of stable multicharged cations and, in particular, a dication can only be suggested by analogy with valence-isoelectronic TOC **7** and STC **10**.

V.2. NMR and EPR spectroscopic studies

The NMR spectra of the majority of heterocirculenes are difficult to record because of very low solubility of these compounds. In particular, Wynberg and Dopper[33] failed to measure ^{13}C NMR spectra of thia[7]circulenes **13** and **32** – **34**, but recorded their ^1H NMR spectra in carbon disulfide. These spectra show well-known multiplets at 7.6 ppm characteristic of fused sulfur-containing heterocycles.[33] These experimental data refute the assumption that polarized resonance structures are present as an admixture to the ground electronic state of thia[7]circulenes, as it was suggested[1, 33] for corannulene **1**.

Thia[7]circulenes **13** and **33** can undergo electroreduction to form the corresponding radical anions. Taking into account the symmetry, the radical anions of compounds **13** and **33** contain three and four groups of equivalent protons, respectively, as was established by EPR spectroscopy.[33] The proton hyperfine splitting constants (*a*/G) are presented in Fig. 7.

Radical cations of sulflower **9** were also studied by EPR spectroscopy.[21] Only a few solvents dissolve sulflower, among which is trifluoromethanesulfonic acid acting as a strong oxidant. The dissolution in this solvent gives a purple solution (the acid and the starting amorphous sulflower are colourless), and the EPR spectrum shows a broad singlet (*g*-factor 2.008). Most likely, this signal is due to radical cations of sulflower as paramagnetic species, the presence of which accounts for a change in the colour of sulflower upon the dissolution. Our calculations of the anisotropy of the *g*-factor for the radical cation of sulflower **9** by the linear response method[106] gave the positive shift $\Delta g = 0.0099$ in good agreement with the experimental data ($\Delta g = 0.0057$).[21]

Unlike other thiacirculenes, sulflower **9** was characterized also by ^{13}C NMR spectroscopy in the condensed phase under magic angle spinning (MAS) conditions.[107] This technique provides high-resolution spectra. Due to high symmetry of circulene **9**, the ^{13}C NMR spectrum of this compound shows only two signals at δ 125 and 138 ppm assigned to two groups of equivalent C^β and C^α atoms in the inner and outer perimeters of the macrocycle, respectively. The signal at δ 138 ppm is observed also in the ^{13}C NMR spectra of fused di-, tri- and tetratrienes.[108, 109] The signal at δ 125 ppm is not reproduced in the ^{13}C NMR spectra of these solutions. This is attributed to a specific character of the shielding of the nuclei of C^β atoms in the inner antiaromatic COTR due to paratropic ring currents.

The spectroscopic features of unsubstituted tetraoxa[8]-circulenes were poorly studied by ^{13}C and ^1H NMR spec-

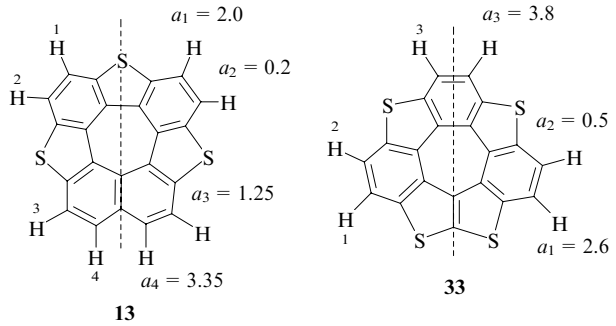


Figure 7. Hyperfine splitting constants (G) for equivalent protons of circulenes **13** and **33**.[33]

troscopy because of low solubility of these compounds, in contrast to alkyl-substituted TOC, which were characterized by ^{13}C and ^{1}H NMR spectroscopy. The most useful information for the estimation of the aromatic character of the macrocycle in TOC is provided by ^{1}H NMR spectroscopy. Unfortunately, it is impossible to draw conclusions about the aromatic properties of the macrocycle in octaalkyltetraoxa[8]circulene **14** based on its ^{1}H NMR spectrum (R = n-$C_{11}H_{23}$)[32,50] because all aromatic protons are replaced, and the ^{1}H NMR spectrum dispalys only multiplets at δ 1.27–3.17 ppm[50] characteristic of aliphatic protons.

The ^{1}H NMR spectra of mixed TOC **15**–**18** (R = n-$C_{11}H_{23}$)[32] show, apart from signals of aliphatic protons at δ 0.9–3.05 ppm, multiplets at δ 7.45–8.5 ppm assigned to different groups of aromatic protons of unsubstituted naphthalene moieties. Signals of aromatic protons at δ 7.68 (s, 4 H) and 7.71 (s, 2 H), 7.60 (s, 2 H) ppm in the ^{1}H NMR spectra of isomeric tetra-*tert*-butyltetraoxa[8]circulenes **21** and **22**, respectively,[64] provide a direct evidence of the aromatic character of the benzene and furan rings in TOC molecules (Fig. 8). The aliphatic hydrogen atoms give characteristic resonance signals at δ 1.70 (s, 36 H) and 1.75 (s, 18 H), 1.70 (s, 18 H) ppm, respectively.

A similar pattern is observed in the ^{1}H NMR spectrum of azatrioxa[8]circulene **11**.[24] Aromatic protons adjacent to the furan ring give a characteristic singlet at δ 7.67 (s, 2 H) ppm, whereas the resonance signal of protons adjacent to the pyrrole ring is slightly shifted upfield: δ = 7.34 (s, 2 H) ppm.

It is interesting to study heterocirculene molecules in terms of the NICS theory, which is often applied to investigate the aromaticity of organic compounds[80] and, in particular, of planar cycloocatatetraenes.[22,23,54–56,80–85,110–114] In terms of the concept of nuclear magnetic resonance, the NICS indices correspond to the absolute values of the magnetic shielding, which are calculated at certain points of the molecule. As a rule, the NICS indices are calculated in the centre of the ring [NICS(0)] and at points above the centre with a step of *n* generally multiple to 1 Å [NICS(*n*)]. The NICS(1) values were recommended[80,81] for the use instead of the NICS(0) indices in order to more correctly take into account π-electronic effects. Significantly negative values of NICS(0) and NICS(1) in the centre of the ring attest to induced diatropic ring currents, which corresponds to the aromaticity, whereas the positive values of NICS indices at these points are indicative of paratropic ring currents, *i.e.*, of antiaromaticity.[80]

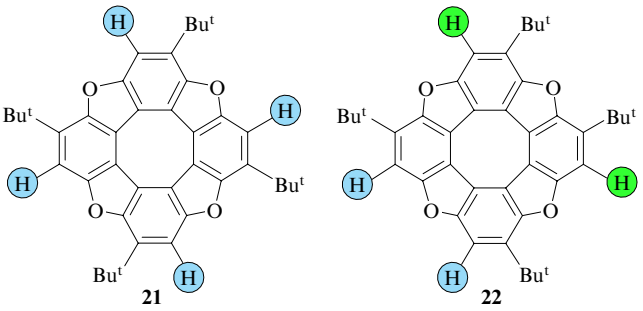


Figure 8. Structures of two regioisomers of tetra-*tert*-butyltetraoxa[8]circulene (groups of equivalent aromatic protons are drawn in different colours).

According to this criterion, it was found that the inner eight-membered ring in most of circulene molecules **7**–**12**,[23,24,52,92,94,115] **15**–**19**,[82,83] porphyrins **23**, **24** (Refs 70 and 71) and hypothetical circulenes **25**, **26**, **29**–**31** (Refs 84, 85 and 89) is characterized by positive values of NICS(0) and NICS(1) (Table 5) and, consequently, has an antiaromatic character. For example, the NICS(0) and NICS(1) indices for tetraoxa[8]circulene molecules calculated in the centre of the eight-membered ring vary in ranges of 6.55–9.23 and 3.79–5.99 ppm, respectively (Fig. 9). In the case of the formation of TOC dications, which were identified in mass-spectrometric experiments, the inner ring retains the antiaromatic character (Fig. 10). However, in the case of the formation of dianions (for example, in the electrochemical reduction), the eight-membered ring acquires the aromatic character, and the dianion becomes 'doubly aromatic'.[22,23] It should be noted that the benzene and furan rings of TOC retain the aromatic character upon double ionization (in the case of the formation of both dications and dianions, see Fig. 10). Therefore, the dianions of TOC and AOC can be considered as systems having 'double' aromaticity and, consequently, they would be expected to be highly stable.

As can be seen in Fig, 9, all benzene rings in neutral TOC molecules are characterized by significantly negative values of NICS(0) and NICS(1), which vary in ranges from −10.53 to −7.56 and from −10.06 to −7.89 ppm, respectively. These values are rather close to the corresponding values for the free benzene molecule. The same conclusion is true also for the naphthalene moieties of TOC as compared with free naphthalene (see Fig. 9). However, the NICS(0) and NICS(1) indices for the free and fused furan rings are

Table 5. Indices NICS (ppm) for the inner COT ring in hetero[8]circulene molecules.

Circulene	NICS(0)	NICS(1)	Ref.	Circulene	NICS(0)	NICS(1)	Ref.
9	5.6	2.4	52, 115	**25a** (*n* = 4)	−3.3 to 6.6	–	85
[**9**]$^{2+}$ (S_1)	35.3	36.0	103	**25a** (*n* = 5)	3.8 to 5.5	–	85
[**9**]$^{2+}$ (T_0)	−1.4	−3.1	103	**26a**	0.3 to 3.4	–	85
10	5.7	3.0	115	**29**	41.5[a]	25.9[a]	89
[**10**]$^{2+}$ (S_1)	36.9	37.9	103	**30a**	35.5[a]	20.8[a]	89
[**10**]$^{2+}$ (T_0)	2.1	−0.2	103	**30b**	−15.0[a]	−55.5[a]	89
23	21.7	–	71	**31**	−35.7[a]	−51.2[a]	89
24 (M = Zn)	61.7	–	70	COT (D_{4h})	30.1	–	81

[a] The *zz* component of the magnetic shielding ($NICS_{zz}$); the *z* axis is perpendicular to the plane of the molecule.

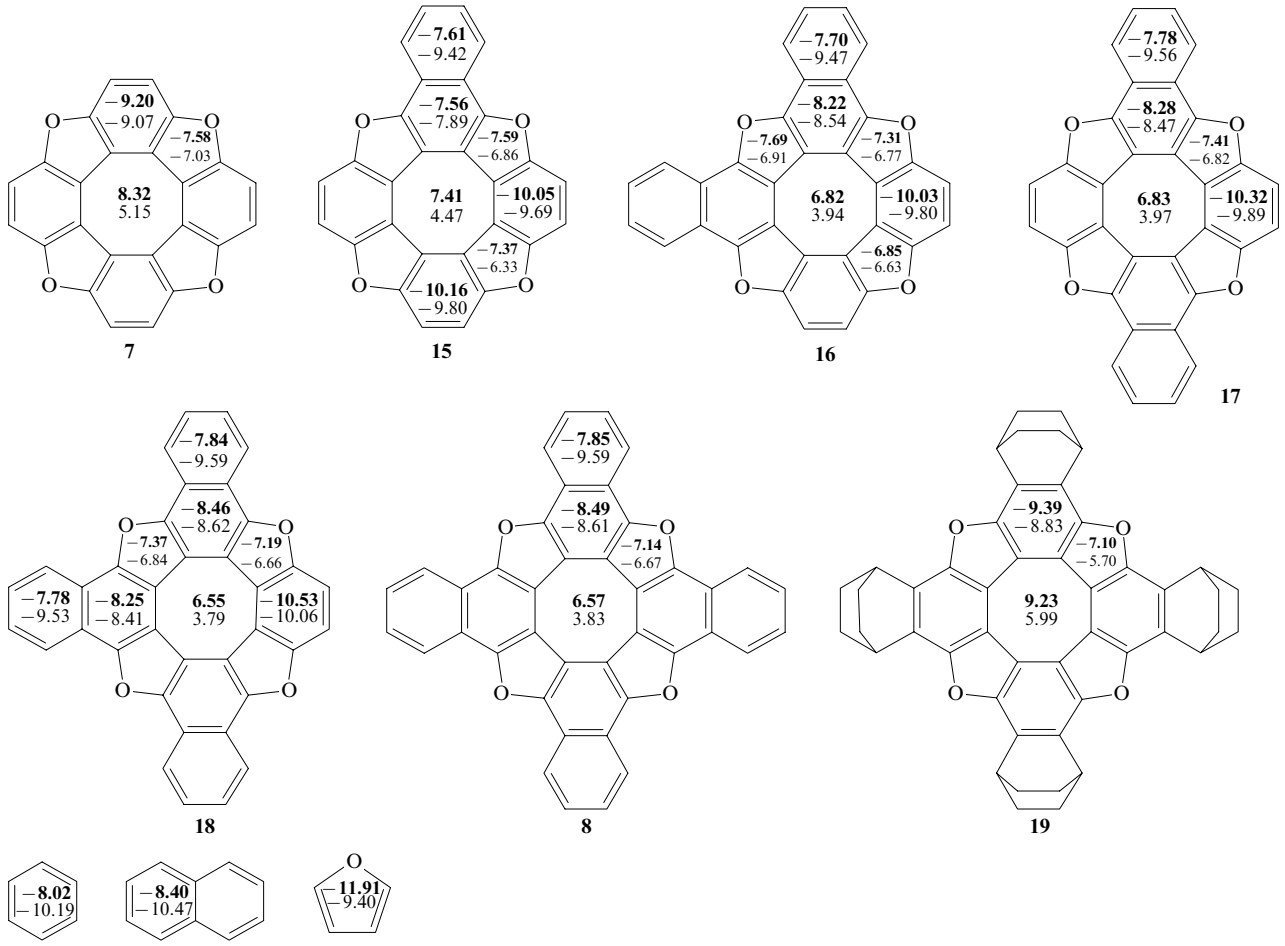


Figure 9. Indices NICS(0) (top row, bold-face type) and NICS(1) (bottom row) in tetraoxa[8]circulene, benzene, naphthalene and furan molecules calculated by the GIAO/B3LYP/6-311 + G(d,p) method.[82]

substantially different in magnitude due to considerable delocalization of the π-system of furan between adjacent benzene rings. Therefore, there is a ribbon-like fused aromatic system of the benzene and furan rings closed around the antiaromatic COTR in TOC molecules. Similar conclusions were drawn by Radenković *et al.*[83] based on calculations of the ring current density in tetraoxa[8]circulenes. Two types of ring currents were found in TOC molecules: paratropic ring currents in the inner COTR and diatropic currents in the outer perimeter, as it was shown in Fig. 6.† In summary, it should be noted that all TOC under consideration conventionally belong to nonaromatic compounds in terms of the magnetic criterion of aromaticity estimated by GIMIC (gauge including magnetically induced current is close to zero), which, on the first glance, is contradictory to low reactivity of these compounds. However, a detailed consideration demonstrates that every chemical transformation of TOC, in particular the addition of reagents at multiple bonds, leads to the disruption of aromatic systems of furan and pyrrole rings, the aromatic character of which is correctly predicted by both theoretical and experimental methods. In our opinion, it is the specificity of the structures of TOC and other planar heterocirculenes that is responsible for their nontrivial electronic structures. These structures have no analogues among known compounds and require further investigation.

It is easy to demonstrate that hetero[8]circulene molecules do not meet the 'annulene in annulene' concept,[116] according to which the outer and inner perimeters should be antiaromatic (because they have $4n$ π-electrons: $n = 2$ for the inner ring and $n = 6$ for the outer one) and characterized by the presence of only paratropic ring currents.

The introduction of pyrrole rings instead of furan moieties into the macrocycle of TOC does not lead to substantial changes in the aromaticity of circulenes (see Fig. 10).[23, 24] The inner eight-membered ring of azacirculenes has antiaromatic character in the case of neutral and dicationic forms (see Fig. 10 *b*,*c*) and acquires aromatic character in the dianion of AOC. The pyrrole, furan and benzene rings retain the aromatic character upon double ionization, as in TOC molecules.

Sulflowers **9** and **10** are isoelectronic analogues of TOC and AOC; however, the aromaticity of the dications of OTC **9** and STC **10** is rather unusual. The calculations showed that the highest occupied molecular orbitals (HOMO) of OTC and STC are doubly degenerate (Fig. 11 *a*), in contrast

† In terms of the magnetic criterion, aromatic systems are those, in which diatropic anticlockwise ring currents dominate, the antiaromatic systems are those, in which paratropic clockwise ring currents play a key role, and the nonaromatic systems are those with the total zero current.

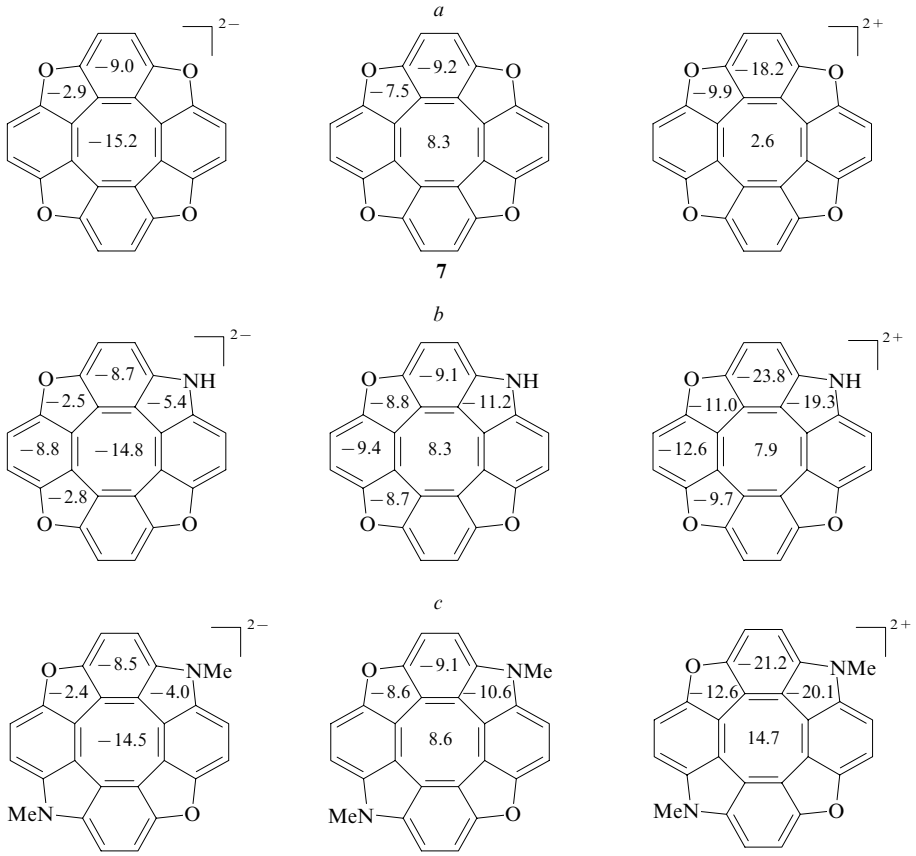


Figure 10. Indices NICS(0) for neutral and doubly ionized tetraoxa[8]circulene (**7**) (*a*), azaoxa[8]circulene (*b*)[23] and *N*,*N*-dimethyldiazadioxa[8]circulene (*c*) molecules.[24]

to tetraoxa[8]circulenes and azaoxa[8]circulenes. Consequently, the double ionization (oxidation) of circulenes **9** and **10** should give rise to dications in the triplet electronic state according to Hund's rule (see Fig. 11 *b*).

This assumption was stated for the first time in the study[95] for sulflower **9**, but no experimental or theoretical justification was proposed. Our calculations by the B3LYP/6-31 + G(d) method proved that the triplet state is the ground state for the dications of sulflowers **9** and **10**, the thiophene and selenophene rings in the triplet state being aromatic (see Table 5), whereas the inner COT ring being nonaromatic [the NICS(0) and NICS(1) indices are close to zero, Table 6]. The singlet state of the dications of sulflowers **9** and **10** (see Fig. 11 *c*) is 4 kcal mol^{-1} higher in energy and, in addition, is fully antiaromatic (*i.e.*, destabilized), including the thiophene and selenophene rings.

The 'double' aromaticity is characteristic also of neutral hypothetical circulene **25a** ($n = 4$; X = Y = N), for which the magnetic NICS criterion implies the aromatic character of the inner COT ring (see Table 5) and the surrounding heterocycles.[85] Evidently, this is due to the predominant contribution of the resonance structure, in which COTR acquires an arbitrary charge 2+ due to the electron-withdrawing environment of the nitrogen atoms. The same conclusion is true for circulenes **30b** and **31** containing strongly electron-deficient boron atoms in the outer perimeter. For the free dication of COTR with the point group of symmetry D_{8h}, the NICS(0) index is −6.4 ppm,[81] which is rather close to −3.3 ppm for circulene **25a** ($n = 4$; X = Y = N). The inner COT ring in circulenes **26a** is nonaromatic, because the planar structure of this ring is distorted and the corresponding NICS(0) indices are close to zero.

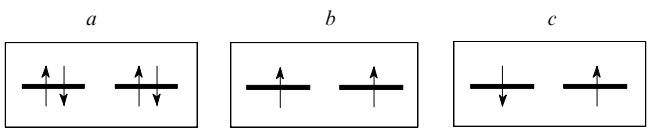


Figure 11. Schematic representation of HOMO of neutral OTC and STC (*a*) and of the triplet (*b*) and singlet (*c*) states of their dications.

Partially annulated hetero[8]circulenes (quasicirculenes) belong to the family of planar cyclooctatetraenes, and some quasicirculenes contain alkene protons directly attached to the eight-membered rings.[117–120] Due to this fact, the aromatic properties of these compounds can be studied by ^{1}H NMR spectroscopy. Dehydrohelicenes should be considered as the first synthesized heterocyclic quasicirculenes.[34, 49, 121, 122] The synthesis of these compounds is based on the intramolecular cyclization of the corresponding heterohelicenes,[120] and they are the starting compounds in the synthesis of thia[7]circulenes. More recently, dehydrohelicenes **39** and **40** containing the inner eight-membered core[35, 123] and the cyclic dimer of dithienothiophene **41** (Ref. 92) were synthesized. Unfortunately, these compounds

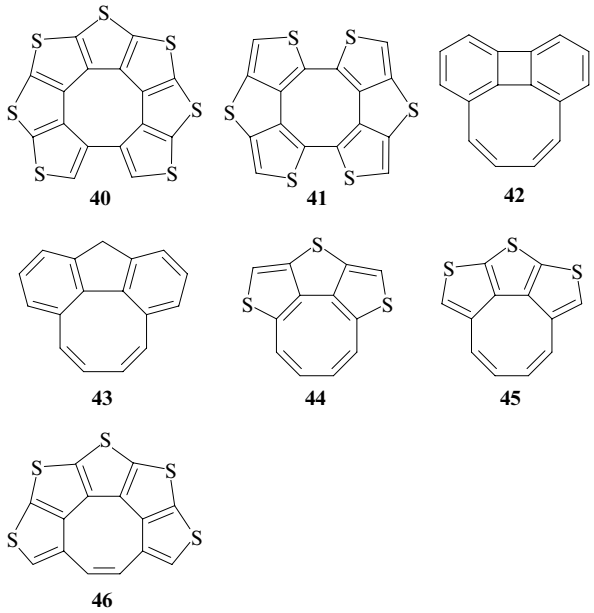
Table 6. Indices NICS (ppm) for five- and six-membered rings in heterocirculenes.

Circulene	NICS(0)	NICS(1)	Ref.	Circulene	NICS(0)	NICS(1)	Ref.
9	−9.8 [a]	−7.4 [a]	52, 115	**25a** (n = 4)	−14.0,[e] −8.9,[e] −6.4 [e]	–	85
[**9**]$^{2+}$ (S_1)	117.1,[a] 129.4 [a]	109.3,[a] 119.9 [a]	103	**25a** (n = 5)	−14.5,[e] −6.9,[e] −2.8 [e]	–	85
[**9**]$^{2+}$ (T_0)	−5.7 to −12.4 [a]	−4.2 to −10.6 [a]	103	**26a**	−14.2,[e] −7.6,[e] −4.1 [e]	–	85
10	−9.8,[a] −9.1 [b]	–	115	**29** [f]	46.6,[g] 19.4 [d]	19.9,[g] −1.8 [d]	89
[**10**]$^{2+}$ (S_1)	141.5,[a] 124.9 [a]	130.3,[a] 116.4 [a]	103	**30a** (see [f])	72.5,[g] 25.1 [a]	42.1,[g] −0.3 [a]	89
	129.4 [b]	124.2 [b]		**30b** (see [f])	20.1,[g] 20.3 [g]	−7.7,[g] −7.7 [g]	89
[**10**]$^{2+}$ (T_0)	−8.0,[a] −9.72 [a]	6.7,[a] 8.4 [a]	103	**31** (see [f])	6.5,[g] −1.0 [h]	−32.6,[g] −34.5 [h]	89
	−5.2 to −13.1 [b]	−3.8 to −11.3 [b]					
23	−4.8,[c] −5.2 [d]	–	71				

[a]Thiophene; [b] selenophene; [c] pyrrole; [d] benzene, [e] X,Y = N, P, As; [f] only the zz component of the magnetic shielding tensor ($NICS_{zz}$) is given; the z axis is perpendicular to the plane of the molecule; [g] borole, [h] cyclopentadienyl.

do not contain alkene protons directly attached to the eight-membered ring, which could give characteristic signals in the ^{1}H NMR spectra indicative of the aromatic properties.

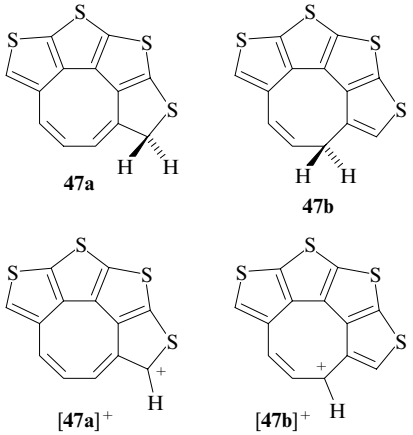
Structures 40–46



Until recently, only two quasicirculenes containing such unsubstituted protons were known. These are hydrocarbons **42** and **43**, in which cyclooctatetraene is annulated to biphenylene [117] and fluorene,[119] respectively. However, in 2013 Aita *et al.*[120] reported the synthesis of the first dithienothiophene-annulated cyclooctatetraene **44** containing unsubstituted alkene hydrogen atoms. It was shown that the signals of these protons appear in the ^{1}H NMR spectrum in the region of 4.4–4.7 ppm, and this is indicative of the antiaromatic character of the inner eight-membered ring. Our quantum chemical calculations at the GIAO/B3LYP/6-311+G(d,p) level of theory confirmed the antiaromatic character of the inner eight-membered ring of quasicirculenes **40** and **42**–**46** based on the positive values of NICS(0) and NICS(1).[118] We also found that the aromaticity of dithienothiophene quasicirculenes strongly depends on the positions of the sulfur atoms in the annulated moiety. For example, the inner COTR of quasicirculene **44** is strictly antiaromatic [NICS(0) = +22.7 ppm, NICS(1) = +17.5 ppm] and its properties are similar to those of free COTR with D_{4h} symmetry [NICS(0) = +30.1].[81] The corresponding values of NICS(0) and NICS(1) for hypothetical quasicirculene **45** are much smaller (+6.2 and +3.5 ppm) and attest to the weak antiaromatic character of COTR. This large difference in the NICS indices for two isomers **44** and **45** is due to distortion of the C=C bond alternation in the inner COTR of quasicirculene **45**. Thus, the calculated bond lengths at the base of three thiophene rings proved to be almost equal (within 0.01 Å), resulting in the violation of the structural criterion of antiaromaticity of COTR, which requires the strict alternation of single and double bonds.

The strict alternation of single and double bonds in the series of quasicirculenes **45**, **46** and **40** containing the odd number of thiophene moieties makes it impossible to predict the existence of the corresponding quasicirculenes containing an even number of thiophene rings. These compounds should contain at least one sp^3-hybridized carbon atom in the annulated moiety or have a cationic structure to meet the condition of planar COTR (as it was shown for structures **47a**,**b** with for thiophene rings).

Structures 47



As follows from the aforesaid, only quasicirculenes **45**, **46** and **40** with an odd number of thiophene rings can exist as planar partially annulated molecules. This is consistent with the fact that only dehydrohelicene **40** has been synthesized, whereas quasicirculenes with an even number of thiophene rings were not prepared. We believe that quasicirculenes **45** and **46** can be synthesized and will have a planar structure.

The behaviour of quasicirculenes **42**–**44** in the double ionization is similar to that of tetraoxa[8]circulene **7**,

azaoxa[8]circulene and diazadioxa[8]circulene (see Fig. 10). For example, the inner COTR in the dianions of quasicirculenes **42**–**44** acquires the aromatic character, in contrast to the dianions of quasicirculenes **40**, **45** and **46**, the inner ring of which has a weakly pronounced antiaromatic (almost nonaromatic) character, as evidenced by small positive values of NICS(0) and NICS(1). Upon double oxidation, all quasicirculenes **40** and **42**–**46** retain the antiaromatic character of COTR and the aromatic character of the annulated moiety. The DFT calculations predict the triplet ground electronic state for the dications of circulenes **40** and **46**.

V.3. IR and Raman spectra of heterocirculenes

Raman and IR absorption spectra provide important information for the analysis of the electronic and geometric structures of hetero[8]circulene molecules.[52, 97]

Vibrational spectra of heterocirculenes were almost not available until recently. For example, in the works by Wynberg and Dopper[1, 33] aimed at the synthesis of thia[7]circulenes, almost no IR spectroscopic data were obtained, except those for intermediates of the synthesis, certain functional groups of which were identified. In particular, intense absorption bands ν(C=O) at 1711 and 1720 cm^{-1} were identified for di(methoxycarbonyl)-trithia[7]circulene (analogue of compound **13** with two methoxycarbonyl groups in one of the two fused benzene rings), and it was shown that aliphatic CH groups are absent.[1] The IR spectrum of tetraoxa[8]circulene **8** is relatively simple (due to high molecular symmetry) and shows a number of unidentified bands (665, 760, 920, 1030, 1060, 1110, 1350, 1425 cm^{-1}).[20] The spectrum of TOC **14** (R = Pr^n)[46] is similar to the spectrum of compound **11** and displays similar bands at 740, 940, 1090, 1230, 1380, 1460, 1690 cm^{-1} and unassigned high-frequency bands at 2860, 2920, 2950 cm^{-1}. Some progress in the assignment of the observed spectral lines of these specific compounds was reached by using a combined approach to the analysis of vibrational spectra of hetero[8]circulenes based on experimental studies and quantum chemical simulation by the DFT method.[97–100] In particular, it was shown that the vibrational spectra of hetero[8]circulenes have a characteristic and, in many aspects, unique set of lines, the frequency and mode of which substantially differ from those of the corresponding lines in the spectra of structure-forming benzene, pyrrole, furan, thiophene and naphthalene molecules.[97–100] These results are extremely important for the analysis of vibronic effects in the UV-Vis absorption and luminescence spectra of hetero[8]circulenes, many of which show vibrational bands.[23, 24, 96]

V.3.a. IR and Raman spectra of octathia[8]circulene

Sulflower **9** was the first heterocirculene, the IR and Raman spectra of which were studied in detail both experimentally and using quantum chemical calculations.[52] The IR spectrum of this compound is very simple (Fig. 12 *a*) due to high symmetry of the molecule (point symmetry group D_{8h}) and the presence of a large number of symmetry-forbidden vibrational modes. Only in-plane e_{1u} and out-of-plane a_{2u} vibrational modes are allowed in the IR spectrum. The totally symmetric in-plane a_{1g} vibrations, as well as the doubly degenerate in-plane e_{2g} vibrations and out-of-plane e_{1g} vibrations, are allowed in the Raman spectrum.[52] There is a total of 66 intramolecular vibrations ($3N-6$, where the number of atoms $N = 24$, all e modes are degenerate) distributed between the symmetry modes as follows:

$$\Gamma_{vib} = 3a_{1g} + 2a_{2g} + 3b_{1g} + 3b_{2g} + 2e_{1g} + 6e_{2g} + \\ + 3e_{3g} + 2a_{2u} + 2b_{1u} + 1b_{2u} + 5e_{1u} + 3e_{2u} + 6e_{3u}$$

In the low-frequency region of the IR spectrum, there are only two absorption bands at 278 and 500 cm^{-1}; the former band has low intensity and was assigned[52] to in-plane e_{1u} vibrations of the macrocycle, and the latter high-intensity band belongs to out-of-plane a_{2u} bending vibrations of the macrocycle. The doublet bands ν(C–S) at 651/657 and 948/958 cm^{-1}, ν(C=C) at 1037, 1110, 1405 cm^{-1} and a very weak out-of-plane vibration band of the macrocycle at 726 cm^{-1} were identified in the medium-frequency range.[52] However, some weak bands in the IR spectrum of sulflower (1345, 979, 864, 797 cm^{-1}) are unidentified and, evidently, belong to symmetry-forbidden vibrations, which are weakly allowed under the effect of intermolecular interactions in the crystal structure. Unlike the IR spectrum, the Raman spectrum of sulflower **9** is more complicated (see Fig. 12 *b*) and is sensitive to the type of the crystal structure.

Thus, the Raman spectrum of single-crystalline sulflower **9** displays a larger number of lines compared to the Raman spectrum of an amorphous sample. Besides, these lines in the spectrum of a crystalline sample are more intense. In the low-frequency range of the Raman spectrum (below 200 cm^{-1}) of amorphous sulflower **9**, the Raman bands are very weak and strongly broadened and, consequently, their maxima cannot be determined with high accuracy. However, in the spectrum of a crystalline sample these lines are well-allowed and identified at 149 and 164 cm^{-1} (see Ref. 52). It was assumed[52] that these lines are due to out-of-plane e_{3g} vibrations of the macrocycle, which are forbidden in the Raman spectra for the point symmetry group D_{8h}, but they are weakly allowed as the molecular symmetry in the crystal lattice decreases.[52]

In-plane vibrations of the macrocycle give a series of Raman lines in the region below 600 cm^{-1}, among which an intense doublet line with maxima at 345 and 338 cm^{-1} should be distinguished. According to the results of the study,[52] the C–S stretching vibrations correspond to medium-intensity bands at 630 and 829 cm^{-1}. In the frequency range > 1000 cm^{-1}, there are lines assigned to different vibrational modes of C=C bonds.[52] The IR and Raman spectra of crystalline sulflower **9** are characterized by Davydov splitting of Raman lines and IR absorption bands[124] caused by resonance interactions between excited molecules due to the excitation transfer from one molecule to another (referred to as a vibrational exciton).[124] The splitting of the lines in the Raman spectrum of crystalline sulflower **9** is rather large (2–4 cm^{-1}).[52] This is evidence of strong intermolecular interactions in the crystalline state.

V.3.b. IR and Raman spectra of tetraoxa[8]circulenes

Tetraoxa[8]circulene **7** is the simplest representative of the class. The IR and Raman spectra of this compound were studied in most detail.[97–100, 125] Circulene molecule **7** has the point symmetry group D_{4h}, consists of 36 atoms and

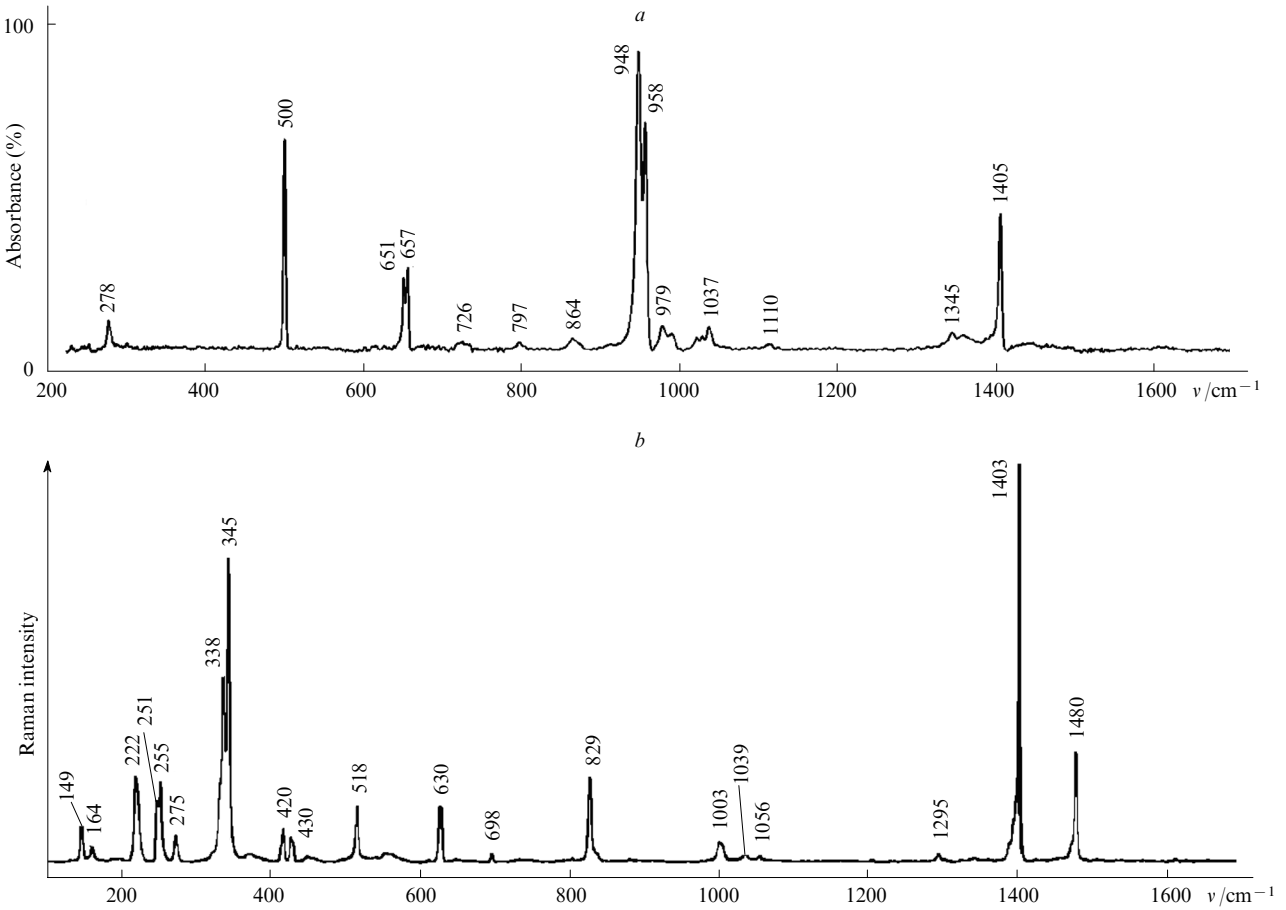


Figure 12. IR spectrum (*a*) and Raman spectrum (*b*) of crystalline octathia[8]circulene **9**.[52]

gives 102 normal vibrations (NV) distributed between the symmetry modes as follows:

$$\Gamma_{vib} = 34\,e_u + 9\,a_{1g} + 8\,a_{2g} + 9\,b_{1g} + 9\,b_{2g} + 16e_g + \\ + 4\,a_{1u} + 4\,a_{2u} + 5\,b_{1u} + 4\,b_{2u}$$

It should be noted that only in-plane e_u vibrations and out-of-plane a_{2u} vibrations are active in the IR spectrum; in-plane a_{1g}, b_{1g}, b_{2g} vibrations and out-of-plane e_g vibrations are active in the Raman spectrum. The same selection rules are valid for normal vibrations of TOC **8** (a total of 174 NV), which are distributed between symmetry modes as follows:

$$\Gamma_{vib} = 15\,a_{1g} + 14\,a_{2g} + 15\,b_{1g} + 15\,b_{2g} + 58\,e_u + 7\,a_{2u} + \\ + 8\,b_{1u} + 7\,b_{2u} + 7\,a_{1u} + 28\,e_g$$

The IR and Raman spectra of all unsubstituted tetraoxa[8]circulenes show bands of characteristic CH vibrations of aromatic rings: stretching vibrations ν(CH) in the frequency range of 3080–3030 cm^{-1}, in-plane bending vibrations δ(CH) in the range of 1240–950 cm^{-1} and out-of-plane bending vibrations below 900 cm^{-1}. It should be noted that in-plane bending vibrations δ(CH) are usually mixed with ν(CO) of furan rings and in-plane bending vibrations of the rings. For example, the most intense line at 1240 cm^{-1} in the Raman spectrum of TOC **7** (Fig. 13) is assigned to NV belonging to bending vibrations δ(CH) strongly mixed with stretching vibrations ν(CO). Out-of-plane bending vibrations γ(CH) in the vibrational spectra of tetraoxa[8]circulenes have low intensity and are virtually absent in the IR and Raman spectra described in our studies.[96–98]

Carbon–carbon stretching vibrations of benzene and furan moieties are usually observed in experimental IR spectra at 1650–1430 cm^{-1} (Ref. 126). The symmetric stretching vibrations do not cause changes in the dipole moments of TOC **7** and **8** and, consequently, they are inactive in the IR spectrum. On the contrary, asymmetric C–C stretching vibrations are active and appear in the experimental IR spectrum of TOC **7** as strong absorption bands at 1421 and 1472 cm^{-1} (Fig. 14) corresponding to NV of the doubly degenerate e_u symmetry.

In the Raman spectrum of TOC **7**, the most intense line belongs to a_{1g}-type NV observed at the experimental frequency of 1670 cm^{-1} and assigned to C=C stretching vibrations of benzene and furan moieties.

Skeletal vibrations of the rings in TOC molecules are associated with the expansion and contraction of all bonds in the benzene and furan rings and in the octatetraene ring and are characterized by strong mixing between these in-plane bending vibrations. This vibrational mode appears as breathing of the above-mentioned rings and is present in doubly degenerate modes observed at the experimental frequency of 870 cm^{-1}.

It is interesting to analyze the IR spectrum of TOC **7** in the triplet excited state. This spectrum can be measured by the time-resolved infrared (TRIR) technique.[127] The TRIR

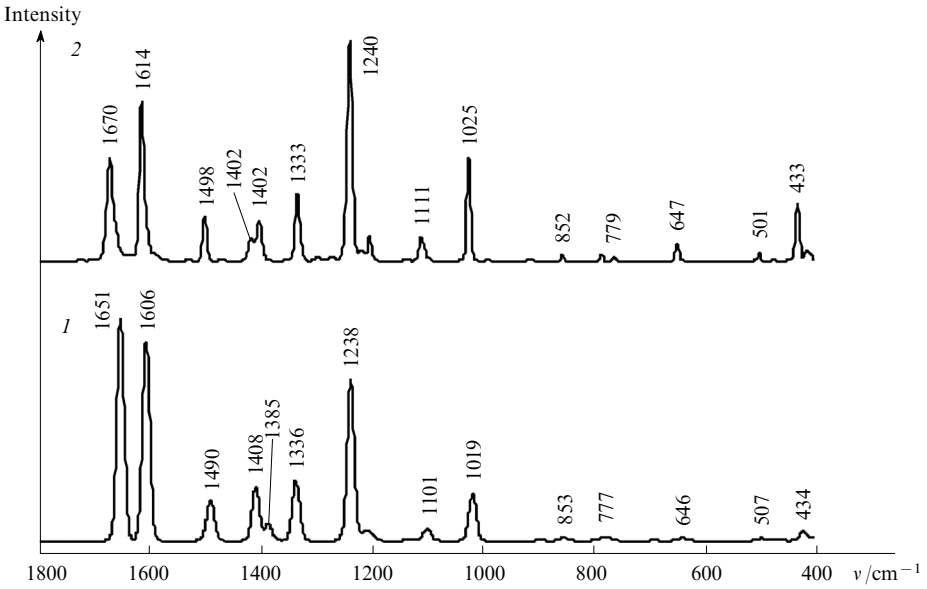


Figure 13. Raman spectrum of tetraoxa[8]circulene **7** calculated at the DFT/B3LYP/6-31G(d) level of theory (*1*) and the experimental spectrum of this molecule (*2*).[125]

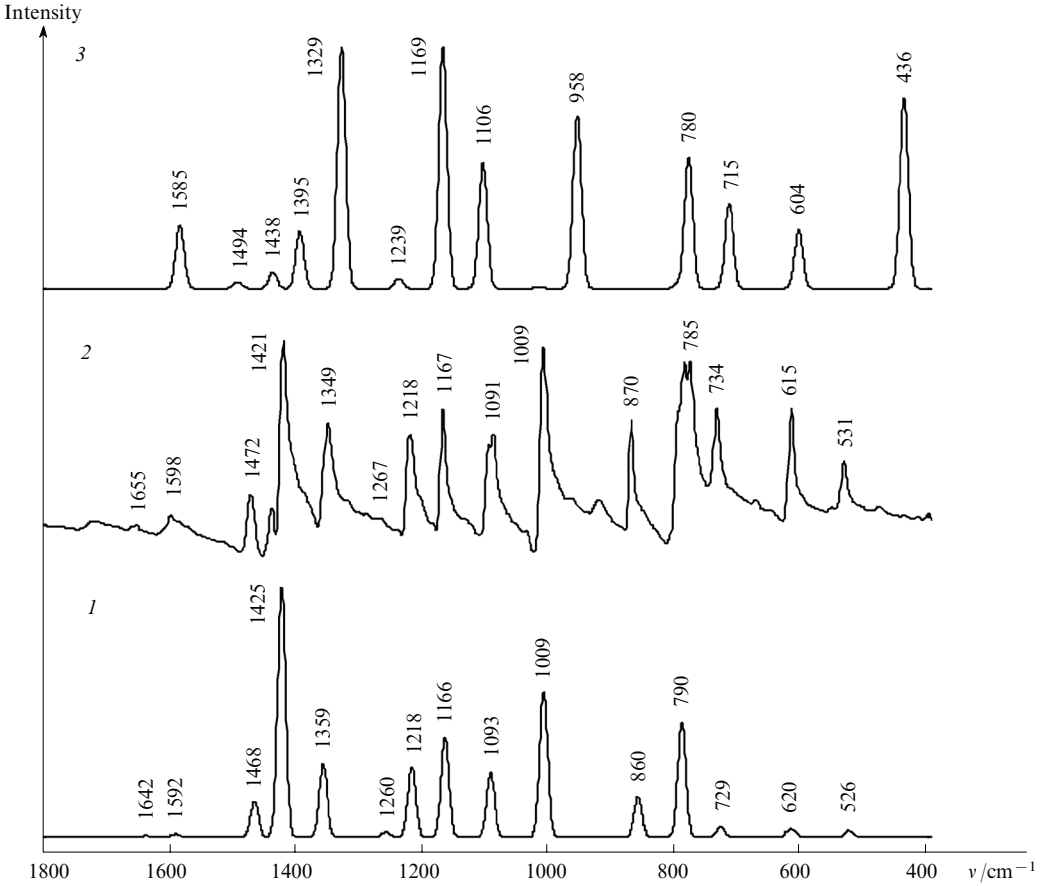


Figure 14. IR spectra of tetraoxa[8]circulene **7**: the calculation of the ground state of the molecule at the DFT/B3LYP/6-31G(d) level of theory (*1*), the experimental IR spectrum (*2*), the calculation of the triplet excited state by the same method (*3*).[125]

method allows for the determination of the time of the formation of the triplet state after the excitation of the molecule. The triplet excited state is short-lived and gives strong absorption in the IR spectral region because the IR spectra of the ground and triplet states are usually substantially different.[127]

Quantum chemical calculations[125] precisely predicted the difference between the IR absorption spectra of the

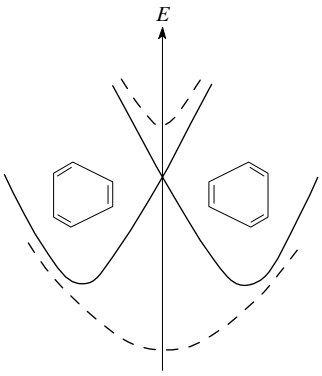


Figure 15. Qualitative scheme of potential energy curves illustrating the difference in the frequencies of Kekule-type vibrations in the ground and excited states of a TOC molecule.[125]

triplet and singlet states of TOC **7**. The excited T_1 state has low symmetry (point symmetry group C_{2v}) unlike the singlet ground state (point symmetry group D_{4h}). Correspondingly, the degeneration of e_g and e_u-type vibrations is absent in this triplet; these vibrations are frequency-split (point symmetry group C_{2v}) and the selection rules for these vibrations are different. The largest frequency shifts in the IR spectrum of triplet TOC **7** are observed for NV corresponding to in-plane bending vibrations of benzene rings. Thus, Kekule-type vibrations in the singlet ground state have a lower frequency (1359 cm^{-1}) compared with the corresponding vibrations in the triplet atate (1395 cm^{-1}), but their intensity is higher in the ground state. As can be seen in the qualitative scheme of potential energy curves (Fig. 15) with different curvature in the upper- and low-lying states, the frequencies of Kekule-type vibrations in the triplet excited state lie at a higher energy compared with the singlet ground state of the TOC molecule.[125]

V.3.c. IR and Raman spectra of azaoxa[8]circulenes

The vibrational spectra of circulenes **11** and **12** consisting of 94 and 104 atoms show 276 and 306 normal modes, respectively, which are distributed in the point symmetry group C_s among the symmetry modes a' and a''. Almost all normal modes that give the observed lines in the Raman spectra are in-phase and totally symmetric (a'). Normal vibrations of a'' symmetry are more IR-active. Four NV ν(CH) of benzene moieties belong to C–H stretching vibrations in the Raman spectrum of circulene **11**, and only two of them are rather active in Raman spectra and appear in the experimental spectrum as a weak doublet at 3091 and 3076 cm^{-1} (Fig. 16).[100] Similar doublet lines are observed in the IR and Raman spectra of diazadioxa[8]circulene **12** (IR, 3070 and 3048 cm^{-1}; Raman, 3089 and 3049 cm^{-1}; see Figs. 16 and 17, respectively).[128] In-plane CH bending vibrations δ(CH) of aromatic rings are not themselves individual normal modes and, in most cases, are mixed with stretching vibrations ν(CO), ν(CN) and ν(CC). In the experimental Raman spectrum of circulene **11**, the contribution of vibrations δ(CH) is observed in the lines at 1257, 1198, 1134 and 1034 cm^{-1}. These corresponding

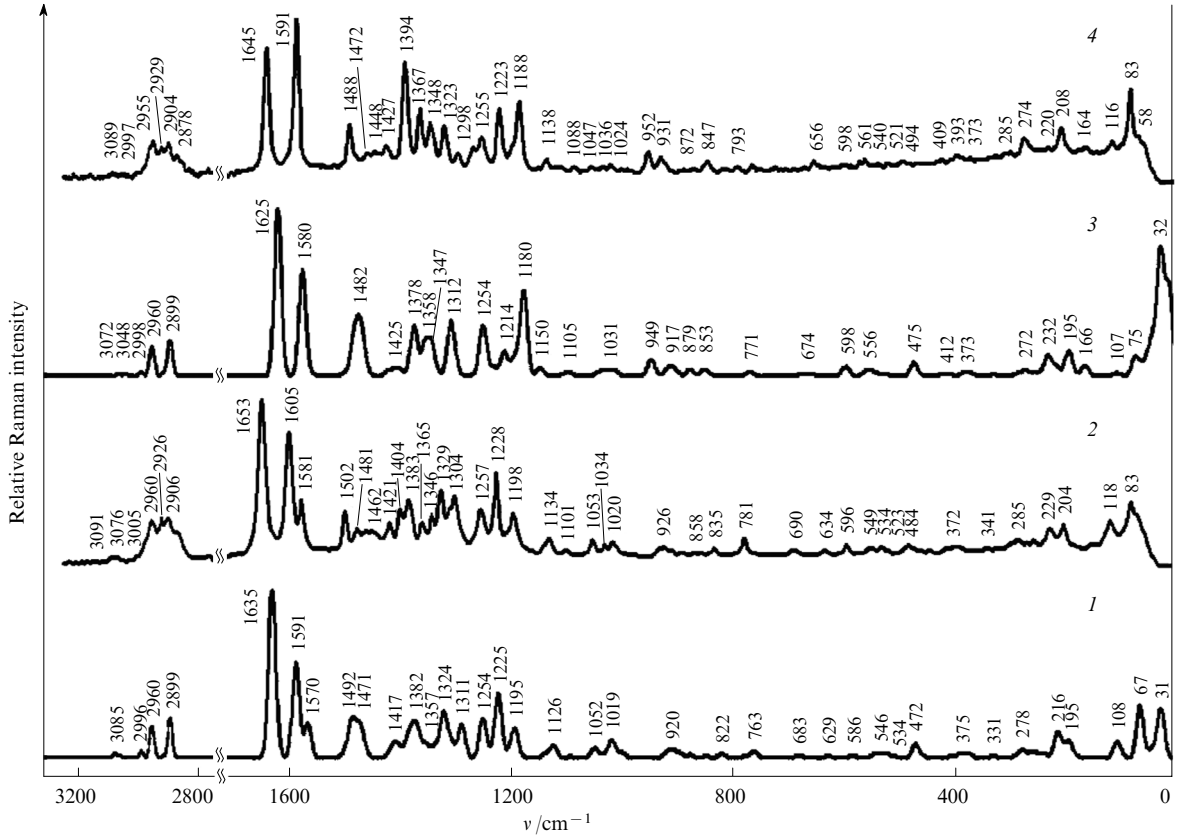


Figure 16. Raman spectra of azaoxa[8]circulenes **11** (*1*, *2*) and **12** (*3*, *4*) calculated at the DFT/B3LYP/6-31G(d) level of theory (*1*, *3*) and the experimental spectra (*2*, *4*).[128]

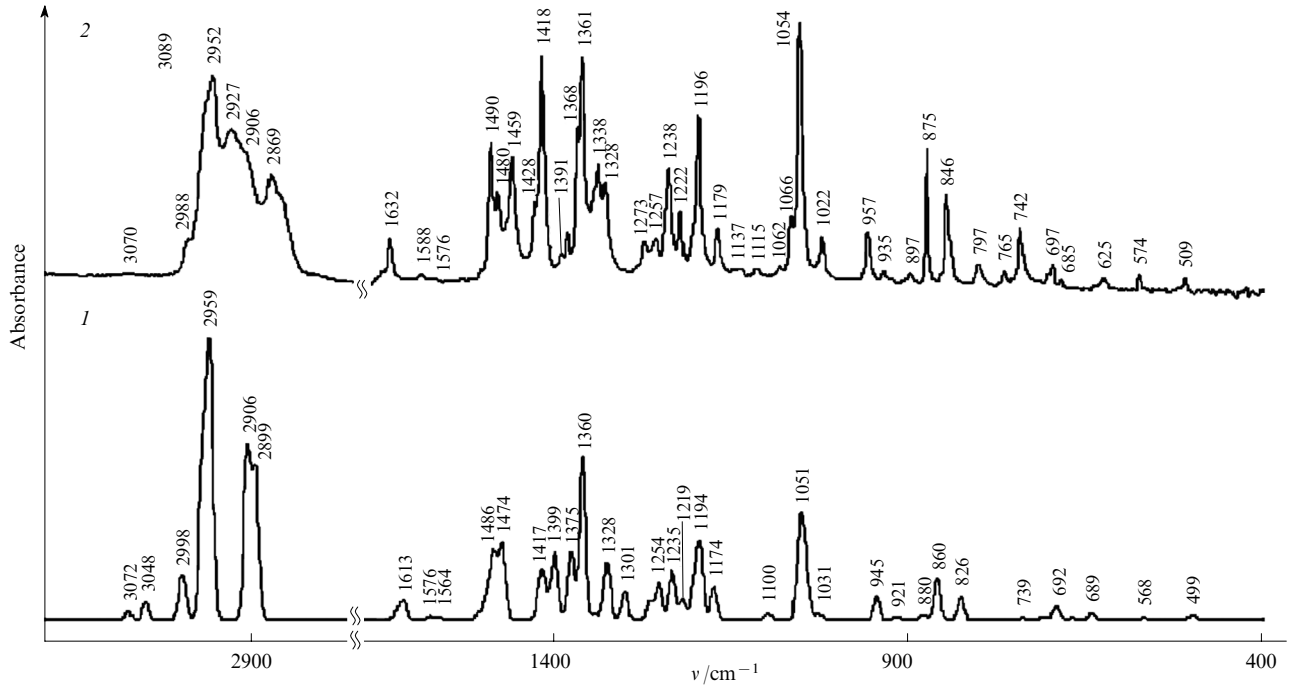


Figure 17. IR spectrum of diazaoxa[8]circulene **12** calculated at the DFT/B3LYP/6-31G(d) level of theory (*1*) and the experimental spectrum (*2*).[128]

vibrations appear as experimental lines at 1255, 1188, 1138 and 1047 cm^{-1} in the Raman spectrum of diazadioxa[8]circulene **12**. The IR spectra of azaoxa[8]circulenes show lines of mixed vibrations δ(CH) in the same range (1254–1044 cm^{-1}). Since out-of-plane CH bending vibrations do not cause changes in polarizability, they are weakly active and are not observed in the Raman spectrum. However, these vibrations appear as medium-intensity bands with maxima at 848 and 846 cm^{-1} in the IR spectra of circulenes **11** and **12**, respectively.

Stretching vibrations of aromatic rings ν(CC) were identified in the experimental Raman spectra of azaoxa[8]-circulenes in the region of 1653–1329 cm^{-1}, the line at 1653 cm^{-1} being the most intense one in the Raman spectrum of circulene **11**. In the IR spectra, this vibrational mode appears as weak bands in the region of 1632–1576 cm^{-1} (see Fig. 17). In the IR and Raman spectra of circulenes **11** and **12**, Kekule-type stretching vibrations ν(CC) are observed in the narrow frequency region of 1340–1320 cm^{-1} and they overlap with other broadened vibrational lines due to low intensity.

In-plane skeletal bending vibrations of benzene and naphthalene moieties are observed as ring-breathing modes and their bending modes. Many of these modes are mixed with other vibrational modes, generally with ν(CO) and(or) δ(CH). The in-phase breathing of all benzene rings in the Raman spectra of circulenes **11** and **12** was assigned to experimental lines at 1228 and 1223 cm^{-1}; the in-phase breathing of the whole macrocycle is observed at 484 and 494 cm^{-1}. In the IR spectra of azaoxa[8]circulenes, the breathing modes are weakly active and overlap with more intense bands.

Azaoxa[8]circulenes differ from tetraoxa[8]circulenes studied earlier[97–100,125] in that they contain pyrrole moieties. Therefore, vibrations of pyrrole moieties are worthy of special analysis. Heteroaromatic compounds of pyrrole and furan groups usually give three Raman lines belonging to C=C stretching vibrations at 1580, 1490 and 1400 cm^{-1} (Ref. 126). In the Raman spectrum of circulene **11**, the first of these lines ($C^{\beta}-C^{\beta'}$ stretching vibration of pyrrole) completely overlaps with C=C bands of benzene rings. The second and third lines are shifted to lower frequencies and appear at 1462 and 1383 cm^{-1}. In the Raman spectrum of diazadioxa[8]circulene **12**, the $C^{\beta}-C^{\beta'}$ stretching vibrations form a strong line at 1394 cm^{-1}. In the IR spectra of azacirculenes, $C^{\beta}-C^{\beta'}$ vibrations do not form individual bands and are mixed with other vibrational modes. For example, in the spectrum of compound **12** ν($C^{\beta}-C^{\beta'}$) vibrations give contributions to weak bands at 1632 and 1257 cm^{-1}, a medium-intensity band at 1238 cm^{-1} and a very strong band at 1054 cm^{-1} (see Fig. 17). The asymmetric $C^{\alpha}=C^{\beta}$ stretching vibrations are weakly active in Raman spectra of azacirculenes, except for the band at 1360 cm^{-1} in the spectrum of circulene **12**. Besides, the $C^{\alpha}=C^{\beta}$ bonds of pyrrole and furan moieties are simultaneously C=C bonds of benzene rings. Therefore, it is not always possible to treat these vibrations separately. In the IR spectra of circulenes **11** and **12**, $C^{\alpha}=C^{\beta}$ stretching vibrations of pyrrole rings give contributions to bands in the range of 1420–1150 cm^{-1}. The C–O stretching vibrations in the IR and Raman spectra of azaoxa[8]circulene molecules are usually mixed with bending vibrations δ(CH), in-plane ring bending vibrations and other vibrational modes in the range of 1390–950 cm^{-1}.

In the IR and Raman spectra of azacirculenes, characteristic lines of macrocycles are overloaded with vibrations of alkyl substituents;[23,24] however, quantum chemical calculations made it possible to precisely identify the positions of 'alkyl' bands[100,128] and separate them from the observed vibrational spectra.

V.3.d. Conversion of vibrational activity to Raman intensity

The activities of normal modes (S_i) in Raman spectra calculated by the density functional theory [73–76] are not identical to the experimentally observed Raman intensities (I_i) because the calculations do not take into account the laser excitation frequency and the real ambient temperature. The activity of NV observed in the Raman scattering is calculated using the polarizability derivative of the electron shell. Recall that in the density functional theory all parameters of electron shells are calculated *ab initio* simultaneously with the total energy minimization using the specified functional. Therefore, the calculated Raman spectra in the coordinates of activity cannot be directly compared with the experimental Raman spectra. In addition, a considerable drawback of the calculated Raman spectra is a substantial underestimation of the activity of low-frequency vibrations, which are often very active in the observed Raman spectra of azaoxa[8]circulenes [100, 128] and tetraoxa[8]circulenes.[97, 99]

Equation (2) for the conversion of the Raman activity (S_i) to the corresponding intensity (I_i) of the ith NV has been proposed.[129, 130] We adjusted this equation for calculations of the Raman spectra of azaoxa[8]circulenes [100, 128] and tetraoxa[8]circulenes.[99] The results of calculations using this equation are in good agreement with the experimental spectra.

$$I_i = \frac{f(\nu_0 - \nu_i)^4 S_i}{\nu_i[1 - \exp(-hc_0\nu_i/kT)]} \qquad (2)$$

where ν_0 is the laser excitation frequency (we used a Nd : YAG laser emitting at 9398.5 cm^{-1} with 300 mW initial power; a germanium diode cooled to 77 K served as a detector), ν_i is the frequency of the ith NV (cm^{-1}), c_0 is the velocity of light in vacuum (2.9979×10^{10} cm s^{-1}), h is Planck's constant (6.6261×10^{-27} erg s), k is the Boltzmann constant (1.3806×10^{-16} erg K^{-1}) and f is the conversion coefficient of the intensity. The calculated values of I_i are usually expressed in parts of unity to compare them with the corresponding normalized experimental spectra.

An analysis of Eqn (2) shows that the term $\exp(-hc_0\nu_i/kT)$ exponentially decreases with increasing vibrational frequency ν_i and gives a considerable contribution (>0.1) at ν_i not higher than 476 cm^{-1}. This is why the calculated intensities I_i of low-frequency Raman lines are an order of magnitude higher (and sometimes even larger) than the corresponding values of the activity S_i. In the other part of the Raman spectrum (from 477 to 4000 cm^{-1}), the term $\exp(-hc_0\nu_i/kT)$ is so small that it can be ignored and the denominator of Eqn (2) can be assumed to be equal to ν_i. Therefore, the term $(\nu_0 - \nu_i)^4$, which rapidly decreases with an increase in ν_i, is a key factor that determines the absolute value of I_i in the medium-frequency range; the S_i/ν_i ratio (if the exponential term is ignored) is a minor factor that determines the Raman line intensity and almost disappears at $S_i > 100$ $Å^4$ $(amu)^{-1}$ (amu is atomic mass unit).

V.4. UV-Vis absorption and luminescence spectra of hetero[8]circulenes

UV-Vis absorption spectra of heterocirculenes were described in detail. In particular, the UV-Vis absorption spectra of thia[7]circulenes **13** and **32–34** in chloroform [33] display a pronounced vibrational structure similar to that observed for dehydrohelicenes.[122] The first long-wavelength absorption maximum of circulenes **13** and **32–34** undergoes a red shift, on the average, by 20 nm with respect to the corresponding band of dehydrohelicenes. In addition, the absorption spectra of thia[7]circulenes are poorly sensitive to the number of thiophene rings in the macrocycle.

V.4.a. Absorption spectra of octathia[8]circulene

In contrast to thia[7]circulenes, the absorption spectra of octathia[8]circulene **9** do not display vibrational structure (Fig. 18),[52, 95] but these spectra are highly sensitive to the type of the crystal structure. Thus, amorphous circulene **9** does not absorb in the visible part of the spectrum and has a white colour. The absorption spectrum of this compound shows two intense bands with maxima at 206 and 244 nm (see Fig. 18). However, single-crystalline sulflower **9** is red-coloured due to additional weak absorption bands in the visible part of the spectrum at 416 and 527 nm.[52] Awaga and co-workers [95] attributed the colour of sulflower in thin films ($\sim$500 nm) to the light interference; however, $\sim$10 μm thick microcrystals are also red.[52] Evidently, the colour of crystalline sulflower **9** is not associated with the interference in thin films and is caused by the existence of strong intermolecular interactions,[52, 57] *i.e.*, the absorption in the visible part of the spectrum is due to collective excitations. In the amorphous state, the UV absorption is caused exclusively by isolated molecules, as was established by quantum chemical calculations:[52, 91, 125] the experimental absorption spectrum of amorphous sulflower is almost identical to the calculated absorption spectrum of the isolated molecule.[52, 91, 125] Sulflower molecule **9** is highly symmetric and belongs to the point symmetry group D_{8h}. Therefore, the spectra of this compound obey complex selection rules characterized by numerous forbidden transitions upon electronic excitation. The calculations by the TD DFT method (time-dependent density functional theory) method predict the most intense absorption band at 239 nm assigned to the doubly degenerate $X^1A_{1g} \rightarrow 2^1E_{1u}$ transition,[124] which is related to the maximum of the observed intense band at 244 nm. In addition, there is a clear-cut shoulder calculated at 262 nm ($X^1A_{1g} \rightarrow 1^1E_{1u}$

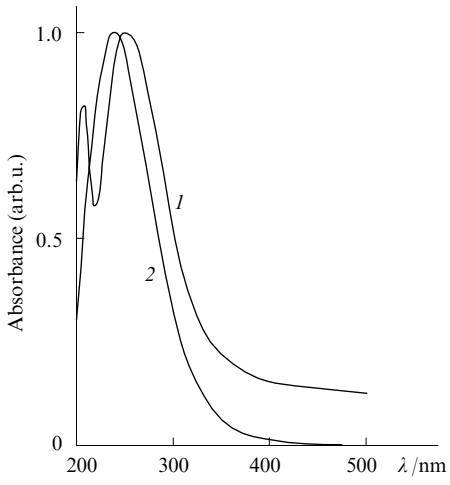


Figure 18. Normalized UV spectra of octathia[8]circulene. (*1*) The band of a freshly sublimed white film (the time of sublimation was 2.5 min),[52] (*2*) the specrum calculated at the TD DFT/B3LYP/6-31G(d) level of theory.[125]

transition)[125] corresponding to the band profile at 277 nm determined by the computer deconvolution of the observed absorption profile[52] (the deconvolution is not shown in Fig. 18).

A weak overtone of the computer deconvolution[52] at 308 nm can be related to the first calculated singlet–singlet $X^1A_{1g} \rightarrow 1^1E_{3g}$ transition at 315 nm.[125] This transition is forbidden and becomes allowed as a results of vibrational electronic coupling and mixing with the $^1E_{1u}$ states due to e_{2u} vibrations. This may account for a low but non-zero intensity of this long-wavelength band.

V.4.b. Absorption spectra of tetraoxa[8]circulenes and azaoxa[8]circulenes

The UV-Vis absorption spectrum of tetraoxa[8]circulene **7** in dichloromethane[32,96] is presented in Fig. 19 (curve *3*). The spectrum shows a very weak band with a maximum at 415 nm due apparently to the first electronic transition $X^1A_{1g} \rightarrow 1^1A_{2g}$.[96,125] In the region of 358–376 nm, there are two more intense bands, and a very intense band with a maximum at 264 nm is observed in the UV region of the spectrum. On the UV border of this spectrum, a growing medium-intensity band is observed (see Fig. 19).

Based on quantum chemical calculations at the TD DFT/B3LYP/6-31G(d) level of theory, it was established that the first transition $X^1A_{1g} \rightarrow 1^1A_{2g}$ in the UV-Vis spectrum of TOC **7**, which we relate to the experimental maximum at 415 nm, occurs exactly at 415 nm and corresponds to the excitation from the highest occupied molecular orbital of $2b_{2u}$ symmetry to the lowest unoccupied molecular orbital (LUMO) of $2b_{1u}$ symmetry (Fig. 20).[96,125] This transition at 415 nm is forbidden in the electric dipole approximation and is allowed as a magnetic dipole transition. It has a relatively large magnetic moment of the transition $\mu_z = 3.4\ \mu_B$ (μ_B is Bohr magneton). The corresponding oscillator strength (f) for the purely magnetic transition is 1.1×10^{-7}. This value cannot explain the observed intensity, the experimental estimate of which is

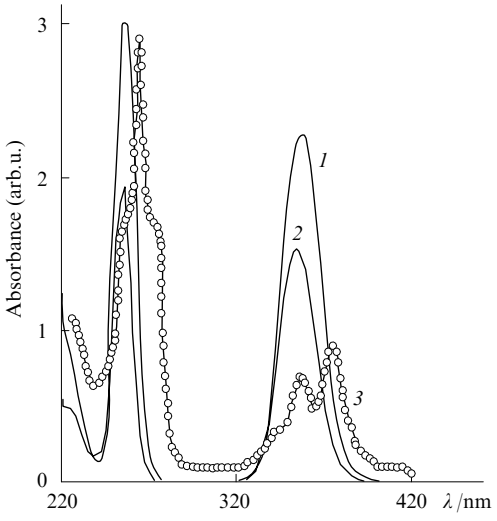


Figure 19. Normalized UV-Vis spectra of tetraoxa[8]circulene **7**.[96] (*1*) Calculated at the TD DFT/B3LYP/6-31G(d) level of theory taking into account the solvent effect (CH_2Cl_2), (*2*) calculated in the vacuum approximation, (*3*) experimental.

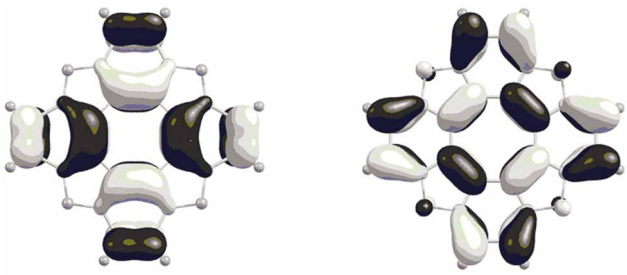


Figure 20. Frontier molecular orbitals of tetraoxa[8]circulene **7** calculated by the DFT/B3LYP/6-31G(d) method.[96]
The transition between these orbitals gives a weak (forbidden) band at 415 nm.

3–4 orders of magnitude higher ($f \approx 10^{-3}$). Evidently, this transition is due to the vibrational electronic coupling between the $^1A_{2g}$ and ^1E_u states due to e_u vibrations.

The $X^1A_{1g} \rightarrow {}^1E_u$ transitions are allowed in the electric dipole approximation and are polarized in the plane of the molecule. In terms of the perturbation theory, e_u vibrations lead to the mixing of the $^1A_{2g}$ and ^1E_u states and permit the $X^1A_{1g} \rightarrow 1^1A_{2g}$ transitions to borrow intensity from the allowed doubly degenerate $X^1A_{1g} \rightarrow {}^1E_u$ transition. Therefore, the $S_0 \rightarrow S_1$ transition becomes weakly allowed and is observed in the experimental absorption spectrum due to which fluorescence of TOC **7** is weakly allowed and is attributed to the break-up of two closely spaced singlet excited states of ^1E_u and $^1A_{2g}$ symmetry with a total quantum yield $\Phi = 0.09$.[32,96] The next two more intense absorption bands of TOC **7** (358 and 376 nm) are due to the $X^1A_{1g} \rightarrow 1^1E_u$ electronic transition. Our calculations imply only one allowed transition in this region. Therefore, we assigned these bands to a vibronic progression. The 0–0 vibrational electronic transition at 376 nm is more intense than the 0–1 transition at 358 nm. The absorption spectrum of TOC **7** shows also the 0–2 transition as a weak inflection in this absorption band (~342 nm).[125] This vibronic progression is characterized by an approximately equal 0.16 eV interval and should correspond to the totally symmetric a_{1g} vibration at 1240 cm^{-1} [the vibrational mode ν_{71} is assigned as δ(CH)/ν(CO), in-phase ν(CC)].[97,125]

As in the UV-Vis spectrum of the simplest TOC **7**, the vibrational structure is pronounced in the spectra of other symmetrical tetraoxa[8]circulenes. An example is the absorption spectrum of circulene **17** (R = H), in which bands at 412 and 390 nm are clearly seen (Fig. 21), but only one $^1A_g \rightarrow {}^1B_{1u}$ electronic transition was found in this region by calculations. Therefore, we assigned the second absorption band (390 nm) to the 0–1 vibronic transition.

Similar spectroscopic properties are characteristic of circulene **16** in the absorption region of 320–400 nm. The characteristic feature of this spectrum is the presence of two closely spaced electronic transitions calculated at 368 and 389 nm, which correspond to one broad absorption band with a maximum at 377 nm (see Fig. 21). In the experimental spectrum, each transition has a pronounced vibrational structure: more intense 0–0 bands and less intense 0–1 vibronic satellites are clearly seen. Since compounds **16** and **17** are isomers, their UV-Vis absorption spectra are on the whole similar, but the vibrational structure of the spectrum

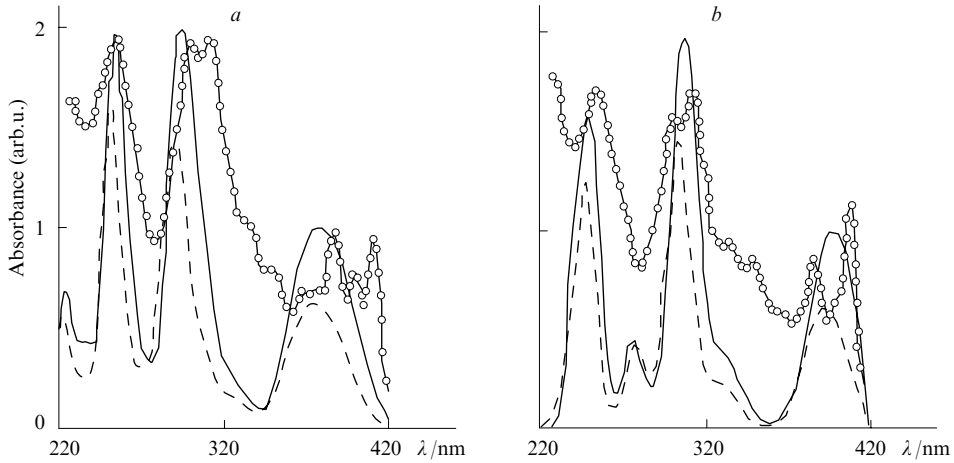


Figure 21. Normalized UV-Vis spectra of tetraoxa[8]circulenes **16** (*a*) and **17** (*b*).[32]
The solid line indicates the spectrum calculated by the TD DFT/B3LYP/6-31G(d) method taking into account the solvent (CH_2Cl_2) effect; the dashed line represents the spectrum calculated in the vacuum approximation; points indicate the experimental data.

of **16** is less pronounced. For circulenes **16** and **17**, the first electronic transition is symmetry-allowed and the fluorescence quantum yields of these compounds are rather high (Φ = 0.51 and 0.83, respectively). The fluorescence spectra of all tetraoxa[8]circulenes (Fig. 22 presents their comparison) and of azaoxa[8]circulenes **11** and **12** (Ref. 24) also have a pronounced vibrational structure and are mirror symmetric[32,96] with respect to the corresponding absorption spectra, thus indicating insignificant changes in the molecular structure and vibrational frequencies in the excited state of TOC molecules.

It should be noted that the Stokes shift for most TOC is rather small (TOC **15**–**18**), whereas the corresponding shift for the simplest TOC **14** is considerably larger (see Fig. 22) due to the specific features of its emission spectrum. Thus, the first electronic transition in the absorption spectrum of TOC **14** at 415 nm is forbidden in the electric dipole approximation and gives almost no contribution to the fluorescence spectrum, whereas the doubly degenerate S_2 state exhibits good fluorescence. At first glance, this is in contradiction to Kasha's rule. However, the kinetics of fluorescence quenching of TOC **14** actually displays two relaxation channels: fast (5.5 ns) and slow (10 ns).[32] These channels apparently correspond to emission from the S_2 and S_1 states, respectively. We performed quantum chemical calculations[96] of the emission spectrum of TOC **7** (analogue of TOC **14** with R = H) taking into account both Franck–Condon and Herzberg–Teller effects and showed that the fluorescence intensity from the S_1 state is weak (but non-zero), while the almost mirror symmetric emission spectrum reflects the vibrational structure of the S_0-S_2 transition with a large Stokes shift (Figure 22 shows the 0–0 and 0–1 bands both in absorption and emission spectra). According to the results of calculations by the TD DFT method, this transition is characterized by a considerable oscillator strength (0.35) responsible for high intensity in the emission. In other TOC molecules (**15**–**18**), the first S_0-S_1 transition is symmetry-allowed and is characterized by a considerable oscillator strength. It should be noted that only a progression of this transition with an intense 0–0 line having a small Stokes shift is observed in the emission spectrum. This is also consistent with high fluorescence quantum yields of all TOC, except compound **14**.

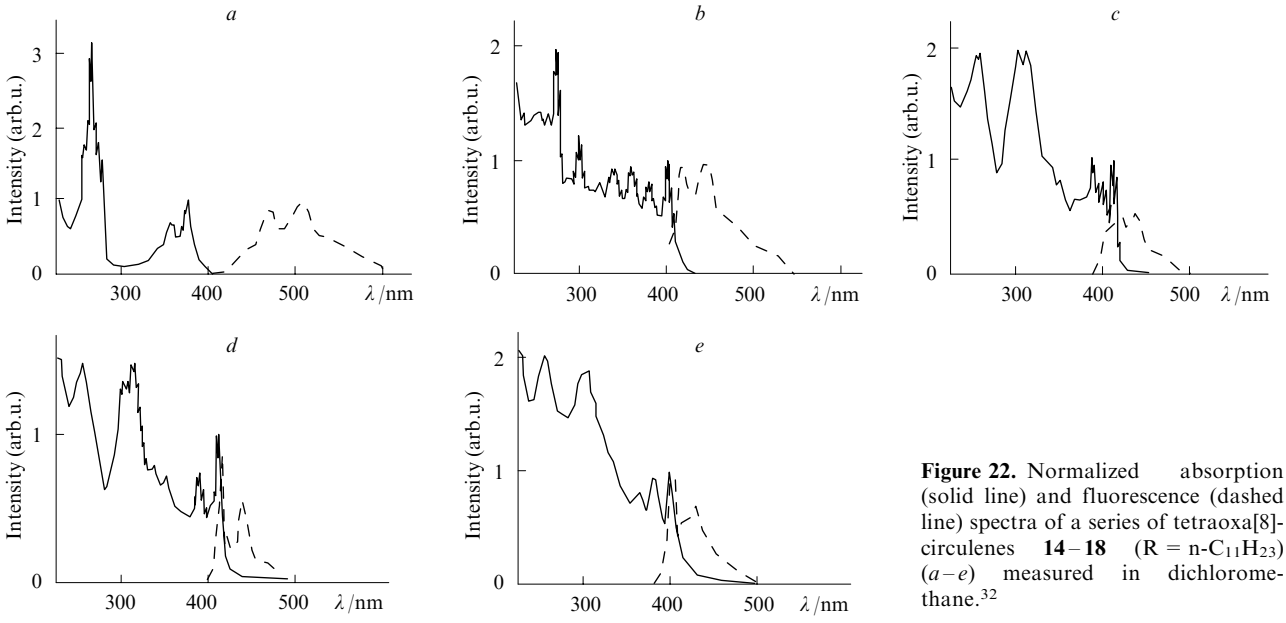


Figure 22. Normalized absorption (solid line) and fluorescence (dashed line) spectra of a series of tetraoxa[8]-circulenes **14**–**18** (R = n-$C_{11}H_{23}$) (*a*–*e*) measured in dichloromethane.[32]

The role of intersystem crossing in the deactivation of the fluorescent state of heterocirculenes, which would lead to the population of the triplet states responsible for phosphorescence, deserves mention here. However, phosphorescence of heterocirculenes is forbidden in most cases even taking into account spin–orbit coupling and can be weakly allowed only due to spin-vibronic perturbations.[96] In addition, heterocirculenes are characterized by a rather large S_1-T_1 gap (>1 eV for OTC and STC).[57] Therefore, the S_1-T_1 conversion is highly improbable, but the population of higher-lying triplet states is quite possible taking into account the spin–orbit coupling and spin-vibronic perturbations.

One of approaches to the improvement of luminescent properties of tetraoxa[8]circulenes is to decrease the symmetry of these molecules by means of functionalization of the outer ring with alkyl substituents or by the replacement of oxygen atoms in the macrocycle by nitrogen atoms. For this purpose, azaoxa[8]circulenes **11** and **12** were synthesized.[23,24] These compounds, unlike TOC **7** and **14**, are characterized by intense absorption in the visible range of 380–450 nm (Fig. 23) and a rather high fluorescence quantum yield ($\Phi = 0.3-0.9$).[23,24]

In order to explain these features, the UV-Vis absorption spectra of azaoxa[8]circulenes **11** and **12** were interpreted by the quantum chemical method at the TD DFT/B3LYP/6-31G(d) level of theory.[75–77] Each molecule belongs to the point symmetry group C_s (ground electronic state $^1A'$). Therefore, the spectrum displays electronic transitions of only two types, *viz.*, $X^1A' \rightarrow {}^1A'$ and $X^1A' \rightarrow {}^1A''$, allowed in the electric dipole approximation.

The first electronic transition in circulenes **11** and **12** is characterized by a rather low intensity, but this transition is manifested as medium-intensity bands at 420 and 419 nm, respectively, in the experimental spectra due apparently to vibronic effects. For comparison, the first electronic transition in the spectrum of *tert*-butyl-substituted TOC **21** (see Fig. 23) is strictly symmetry-forbidden (point symmetry group C_{4h}) and appears in the absorption spectrum as a weak absorption band at 420 nm, like that in the spectrum of unsubstituted TOC **7**.[125]

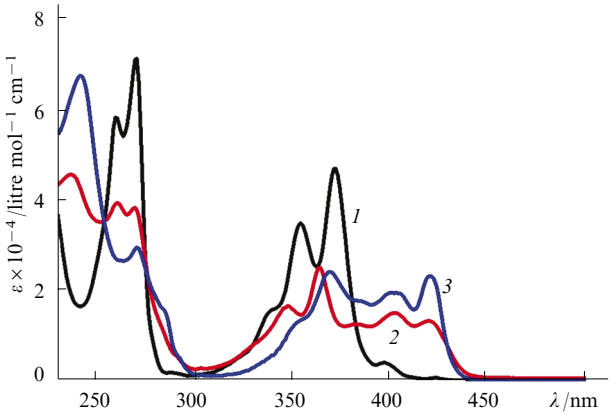


Figure 23. Experimental UV-Vis absorption spectra of tetraoxa[8]-circulene **21** (*1*) and azaoxa[8]circulenes **11** (*2*) and **12** (*3*).[24]

VI. New materials based on hetero[8]circulenes

The main goal of the synthesis of most organic compounds is to design new functional materials with improved properties compared to available analogues. Usually, each new compound is tested for the possible practical application and then the direction of subsequent synthetic works is chosen. Hetero[8]circulenes are not the exception. Thus, thia[8]circulenes **9** and **10** proved to be promising p-type semiconducting materials for organic field-effect transistors (OFET).[22] Unfortunately, the experimental assessment of the performance parameters of OFET based on circulenes **9** and **10** showed low hole mobility at 9.0×10^{-3} and 1.0×10^{-3} cm^2 V^{-1} s^{-1}.[22] However, quantum chemical calculations predicted much higher (by almost three orders of magnitude) hole and electron conductivity: 3.5 and 2.6 cm^2 V^{-1} s^{-1} for sulflower **9**.[131] Such contradictory results require the continuation of research in this field in order to improve the morphology of the materials and the performance characteristics of OFET.

Tetraoxa[8]circulenes are used in practice also as discotic liquid crystals;[50] nevertheless, tetraoxa[8]circulenes hold more promise for the design of organic light-emitting diodes. Such diodes based on TOC **14**–**18** were tested for the first time.[32] The best performance characteristics of OLED were found for TOC **17** (light brightness is 817 cd m^{-2} at a current density of 135 mA cm^{-2} and a power efficiency of 12 V),[32] which correlates well with the highest intensity of the first singlet–singlet electronic transition in TOC **17** as compared to other tetraoxa[8]circulenes,[96] *i.e.*, the fluorescence from the S_1 state for **17** is most well-allowed in the series of circulenes **14**–**18**. It should be noted that the efficiency of OLED based on tetraoxa[8]circulenes is insufficiently high compared to other analogues based on carbazole derivatives, the brightness of which is 15 times higher (reaches 12 500 cd m^{-2}).[132] The efficiency of OLED doped with Ir^{III} complexes[133–138] is even higher (the brightness can be as high as 56 900 cd m^{-2} based on the [Ir(ppy)$_3$] complex, where Hppy is 2-phenylpyridine)[139,140] than that of OLED based on tetraoxa[8]circulenes.[32] This is associated primarily with the insufficiently efficient energy transfer from the (4,4′-*N*,*N*′-dicarbozolyl)biphenyl matrix to tetraoxa[8]circulene molecules.[32] Therefore, the efficiency of OLED based on tetraoxa[8]circulenes can be improved by selecting optimal materials for the matrix and layers with electron and hole conductivity and by employing electron- and hole-blocking materials. Azaoxa[8]circulenes exhibiting higher fluorescence quantum yields ($\Phi = 0.3-0.9$)[23,24] should be more efficient materials for OLED, but the corresponding OLED were not tested as yet.

Great advantages of tetraoxa[8]circulenes, useful for their functionalization, are high molecular symmetry, as well as high thermal and chemical stability. Taking into account that C–H bonds are the main sites for the functionalization in TOC, it was predicted that tetraoxa[8]circulenes can be evolved to form nanotubes [one-dimensional (1D) materials] (for example, **48**) (Fig. 24) and sheet-like nanosized 2D materials[141,142] **49**–**52** (Fig. 25) by means of chemical modifications. This assembly was experimentally observed for porphyrin molecules,[70–72] which form a stable porphyrin sheet (tetramer) **23** with the inner planar cyclooctatetraene core. Another example of the self-assembly of circulenes is the formation of three-dimensional graphene

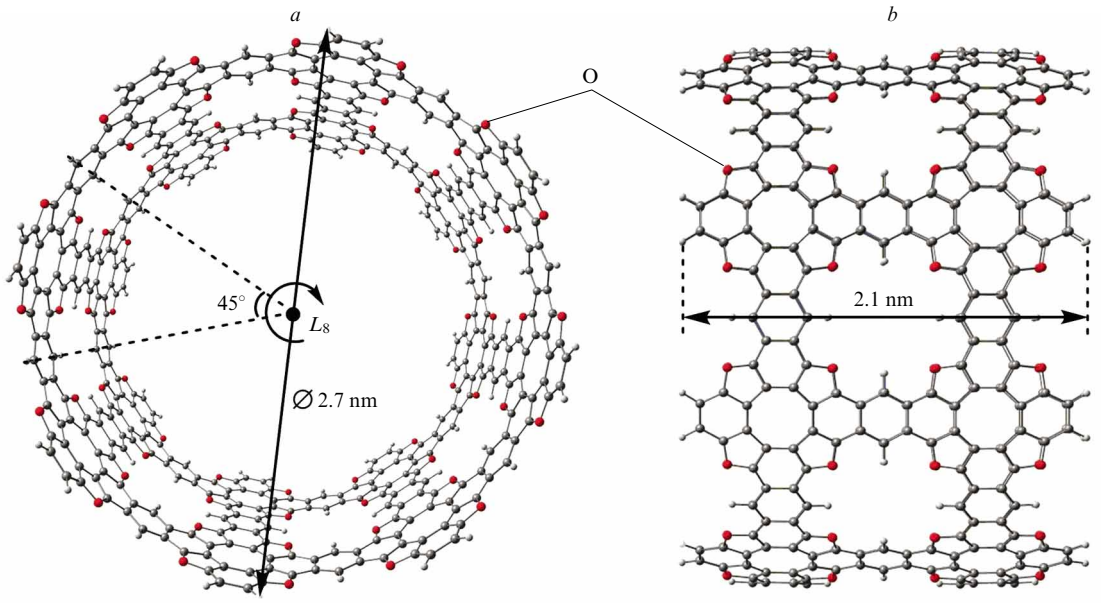


Figure 24. Model of single-walled nanotube **48** (*a*) top view; (*b*) side view.[141]
The assembly is based on the simplest tetraoxa[8]circulene **7**.

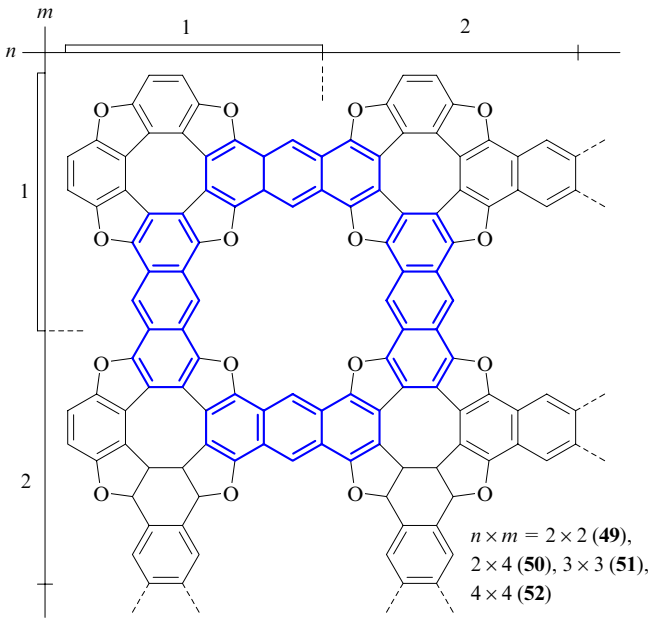


Figure 25. Sheet-like periodic tetraoxa[8]circulenes **49**–**52** (anthracene chromophores are given in blue).[141]

with negative Gaussian curvature (Schwarzite P192)[143] based on saddle-shaped tetrabenzo[8]circulene **6**.[10]

We calculated the heats of formation of hypothetical polymers **48**–**52**. These values attest to high stability of these compounds. The synthesis of these polymers should, apparently, involve the bromination as the first step followed by catalytic polymerization. The strongly exothermic character of the final reaction product gives hope that such interesting structures will be synthesized in the near future.

The synthesis of organic π-conjugated materials **48**–**52** based on tetraoxa[8]circulenes is an important problem from the standpoint of the design of new organic semiconductors. Actually, predicted compounds **48**–**52** have a rather high HOMO energy (~ −4.9 eV)[141] and a very low hole reorganization energy[131, 144–146] (high hole conductivity) characteristic of p-type semiconductors. The characteristic feature of these materials is also intense light absorption in the visible region[141] (at 500 nm), in contrast to simple monomolecular tetraoxa[8]circulenes **14**–**18**.[96] This is primarily due to the presence of conjugated anthracene chromophores in structures **49**–**52** (see Fig. 25). Owing to the presence of large cavities, compounds **48**–**52** are promising hydrogen storage materials, as it was predicted earlier for layered octathia[8]circulene.[93]

VII. Conclusions

The present review clearly shows that hetero[8]circulenes have a specific electronic structure and exhibit aromatic properties due to the fused system of aromatic five- and six-membered rings. The aromaticity stabilizes the planar structure of hetero[8]circulenes and, in particular, the inner cyclooctatetraene ring having an antiaromatic character. Therefore, hetero[8]circulenes are currently the only known stable planar cyclooctatetraenes, the physicochemical properties of which are determined mainly by the aromatic character of the macrocycle. The planar structure of hetero[8]circulenes is responsible for their dense layered packing in the crystalline state. Strong intermolecular interactions cause perturbations in electron shells of adjacent molecules. This, in turn, leads to differences in the UV-Vis spectra of the crystalline and amorphous states of hetero[8]circulenes (crystal chemistry). This difference is particularly pronounced for octathia[8]circulene, which is colourless in the amorphous state and is red-coloured in crystals.

For tetraoxa[8]circulenes and thia[8]circulenes with point symmetry groups D_{4h} and D_{8h}, respectively, the fluorescence from the first excited state is symmetry-for-

bidden. A decrease in the symmetry of hetero[8]circulenes by the functionalization (the synthesis of azaoxa[8]circulenes and unsymmetrical tetraoxa[8]circulenes) results in that the fluorescence becomes allowed and, consequently, new hetero[8]circulenes can be used in organic light-emitting diodes. Therefore, the present review will be helpful and useful for researchers working in the fields of chemical engineering, photophysics and the synthesis of new functional heterocirculenes.

During the preparation of the present review, a series of important studies dealing with this field were reported,[147 – 154] in which new hydrocarbon [152] and heterocyclic [147 – 151, 153, 154] [8]circulenes and 1D and 2D periodic structures based on these compounds were characterized.

References

1. J H Dopper, H Wynberg *Tetrahedron Lett*. **13** 763 (1972)
2. F Diederich, H A Staab *Angew. Chem., Int. Ed. Engl*. **17** 372 (1978)
3. B Kumar, R L Viboh, M C Bonifacio, W B Thompson, J C Buttrick, B C Westlake, M-S Kim, R W Zoellner, S A Varganov, P Mörschel, J Teteruk, M U Schmidt, B T King *Angew. Chem., Int. Ed*. **51** 12795 (2012)
4. B Hajgató, M S Deleuze *Chem. Phys. Lett*. **553** 6 (2012)
5. W E Barth, R G Lawton *J. Am. Chem. Soc*. **88** 380 (1966)
6. R Scholl, K Meyer *Ber. Dtsch. Chem. Ges. B* **65** 902 (1932)
7. K Yamamoto, T Harada, M Nakazaki, T Naka, Y Kai, Sh Harada, N Kasai *J. Am. Chem. Soc*. **105** 7172 (1983)
8. Bharat, R Bhola, T Bally, A Valente, M K Cyrański, Ł Dobrzycki, S M Spain, P Rempała, M R Chin, B T King *Angew. Chem., Int. Ed*. **49** 399 (2010)
9. C-N Feng, M-Y Kuo, Y-T Wu *Angew. Chem., Int. Ed*. **52** 7791 (2013)
10. Y Sakamoto, T Suzuki *J. Am. Chem. Soc*. **135** 14074 (2013)
11. K S Novoselov, A K Geim, S V Morozov, D Jiang, Y Zhang, S V Dubonos, I V Grigorieva, A A Firsov *Science* **306** 666 (2004).
12. S Perumal, B Minaev, H Ågren *J. Chem. Phys*. **136** 104702 (2012)
13. A Hashimoto, K Suenaga, A Gloter, K Urita, S Iijima *Nature (London)* **430** 870 (2004)
14. H W Kroto, J R Heath, S C O'Brien, R F Curl, R E Smalley *Nature (London)* **318** 162 (1985)
15. R Pop, M Medeleanu, M V Diudea, B Szefler, J Cioslowski *Cent. Eur. J. Chem*. **11** 527 (2013)
16. M V Diudea, A E Vizitiu, T Beu, A Bende, C L Nagy, D Janežič *J. Mol. Struct. (THEOCHEM)* **904** 28 (2009)
17. S Iijima *Nature (London)* **354** 56 (1991)
18. J-C Charlier, T W Ebbesen, Ph Lambin *Phys. Rev. B: Condens. Matter* **53** 11108 (1996)
19. P Zhang, V H Crespi *Phys. Rev. Lett*. **83** 1791 (1999)
20. H Erdtman, H-E Högberg *Chem. Commun. (London)* 773 (1968)
21. K Yu Chernichenko, V V Sumerin, R V Shpanchenko, E S Balenkova,V G Nenajdenko *Angew. Chem., Int. Ed*. **45** 7367 (2006)
22. A Dadvand, F Cicoira, K Yu Chernichenko, E S Balenkova, R M Osuna, F Rosei, V G Nenajdenko, D F Perepichka *Chem. Commun*. 5354 (2008)
23. C B Nielsen, T Brock-Nannestad, P Hammershøj, T K Reenberg, M Schau-Magnussen, D Trpcevski, T Hensel, R Salcedo, G V Baryshnikov, B F Minaev, M Pittelkow *Chem. – Eur. J*. **19** 3898 (2013)
24. T Hensel, D Trpcevski, C Lind, R Grosjean, P Hammershøj, C B Nielsen, T Brock-Nannestad, B E Nielsen, M Schau-Magnussen, B Minaev, G V Baryshnikov, M Pittelkow *Chem. – Eur. J*. **19** 17097 (2013)
25. J-E Berg, H Erdtman, H-E Högberg, B Karlsson, A-M Pilotti, A-C Söderholm *Tetrahedron Lett*. **18** 1831 (1977)
26. B Karlsson, A-M Pilotti, A-C Söderholm *Acta Crystallogr., Sect. C* **39** 1273 (1983)
27. F Fouad, S D Bunge, B D Ellman, R J Twieg *Acta Crystallogr., Sect. C* **68** o465 (2012)
28. O Ivasenko, J M MacLeod, K Yu Chernichenko, E S Balenkova, R V Shpanchenko, V G Nenajdenko, F Rosei, D F Perepichka *Chem. Commun*. 1192 (2009)
29. T Fujimoto, M M Matsushita, K Awaga *Appl. Phys. Lett*. **97** 123303 (2010)
30. T Fujimoto, M M Matsushita, K Awaga *J. Phys. Chem. C* **116** 5240 (2012)
31. T Fujimoto, M M Matsushita, K Awaga *Chem. Phys. Lett*. **483** 81 (2009)
32. C B Nielsen, T Brock-Nannestad, T K Reenberg, P Hammershøj, J B Christensen, J W Stouwdam, M Pittelkow *Chem. – Eur. J*. **16** 13030 (2010)
33. J H Dopper, H Wynberg *J. Org. Chem*. **40** 1957 (1975)
34. M B Groen, H Schadenberg, H Wynberg *J. Org. Chem*. **36** 2797 (1971)
35. K Yu Chernichenko, E S Balenkova, V G Nenajdenko *Mendeleev Commun*. **18** 171 (2008)
36. J K Fawcett, J Trotter *Proc. R. Soc. London, Ser. A* **289** 366 (1966)
37. B Kumar, B T King *J. Org. Chem*. **77** 10617 (2012)
38. J C Hanson, C E Nordman *Acta Crystallogr., Sect. B* **32** 1147 (1976)
39. M Shen, I S Ignatyev, Y Xie, H F Schaefer III *J. Phys. Chem*. **97** 3212 (1993)
40. T Liljefors, O Wennerström *Tetrahedron* **33** 2999 (1977)
41. R Salcedo, L E Sansores, A Picazo, L Sansón *J. Mol. Struct. (THEOCHEM)* **678** 211 (2004)
42. L Türker *J. Mol. Struct. (THEOCHEM)* **584** 135 (2002)
43. H Christoph, J Grunenberg, H Hopf, I Dix, P G Jones, M Scholtissek, G Maier *Chem. – Eur. J*. **14** 5604 (2008)
44. H Erdtman, H-E Högberg *Tetrahedron Lett*. **11** 3389 (1970)
45. H-E Högberg *Acta Chem. Scand*. **26** 309 (1972)
46. H-E Högberg *Acta Chem. Scand*. **26** 2752 (1972)
47. H-E Högberg *Acta Chem. Scand*. **27** 2559 (1973)
48. H-E Högberg *Acta Chem. Scand*. **27** 2591 (1973)
49. J H Dopper, D Oudman, H Wynberg *J. Am. Chem. Soc*. **95** 3692 (1973)
50. J Eskildsen, T Reenberg, J B Christensen *Eur. J. Org. Chem*. 1637 (2000)
51. R Rathore, S H Abdelwahed *Tetrahedron Lett*. **45** 5267 (2004)
52. S S Bukalov, L A Leites, K A Lyssenko, R R Aysin, A A Korlyukov, J V Zubavichus, K Yu Chernichenko, E S Balenkova, V G Nenajdenko, M Yu Antipin *J. Phys. Chem. A* **112** 10949 (2008)
53. T Fujimoto, R Suizu, H Yoshikawa, K Awaga *Chem. – Eur. J*. **14** 6053 (2008)
54. P B Karadakov *J. Phys. Chem. A* **112** 12707 (2008)
55. T Nishinaga, T Uto, R Inoue, A Matsuura, N Treitel, M Rabinovitz, K Komatsu *Chem. – Eur. J*. **14** 2067 (2008)
56. T Nishinaga, T Ohmae, M Iyoda *Symmetry* **2** 76 (2010)
57. G V Baryshnikov, B F Minaev, V A Minaeva, V G Nenajdenko *J. Mol. Model*. **19** 4511 (2013)
58. R F W Bader *Atoms in Molecules: A Quantum Theory* (Oxford: Clarendon Press, 1990)

59. E Espinosa, E Molins, C Lecomte *Chem. Phys. Lett.* **285** 170 (1998)
60. E Espinosa, I Alkorta, I Rozas, J Elguero, E Molins *Chem. Phys. Lett.* **336** 457 (2001)
61. X-D Tang, Y Liao, H-Z Gao, Y Geng, Z-M Su *J. Mater. Chem.* **22** 6907 (2012)
62. M J González Moa, M Mandado, R A Mosquera *J. Phys. Chem. A* **111** 1998 (2007)
63. Y Zhao, D G Truhlar *Theor. Chem. Accounts* **120** 215 (2008)
64. T Brock-Nannestad, C B Nielsen, M Schau-Magnussen, P Hammershøj, T K Reenberg, A B Petersen, D Trpcevski, M Pittelkow *Eur. J. Org. Chem.* 6320 (2011)
65. G V Baryshnikov, B F Minaev, V A Minaeva, A T Baryshnikova, M Pittelkow *J. Mol. Struct.* **1026** 127 (2012)
66. M Kastler, W Pisula, D Wasserfallen, T Pakula, K Müllen *J. Am. Chem. Soc.* **127** 4286 (2005)
67. J Zhang, J S Moore *J. Am. Chem. Soc.* **114** 9701 (1992)
68. A-D Schlmter *Adv. Mater.* **3** 282 (1991)
69. T F A De Greff, M M J Smulders, M Wolffs, A P H J Schenning, R P Sijbesma, E W Meijer *Chem. Rev.* **109** 5687 (2009)
70. Y Nakamura, N Aratani, H Shinokubo, A Takagi, T Kawai, T Matsumoto, Z S Yoon, D Y Kim, T K Ahn, D Kim, A Muranaka, N Kobayashi, A Osuka *J. Am. Chem. Soc.* **128** 4119 (2006)
71. Y Nakamura, N Aratani, K Furukawa, A Osuka *Tetrahedron* **64** 11433 (2008)
72. Y Nakamura, N Aratani, A Osuka *Chem.–Asian J.* **2** 860 (2007)
73. P Hohenberg, W Kohn *Phys. Rev., Sect. B* **136** 864 (1964)
74. W Kohn, L J Sham *Phys. Rev., Sect. A* **140** 1133 (1965)
75. A D Becke *J. Chem. Phys.* **98** 5648 (1993)
76. C Lee, W Yang, R G Parr *Phys. Rev. B: Condens. Matter* **37** 785 (1988)
77. M M Francl, W J Pietro, W J Hehre, J S Binkley, M S Gordon, D J DeFrees, J A Pople *J. Chem. Phys.* **77** 3654 (1982)
78. P J Hay, W R Wadt *J. Chem. Phys.* **82** 270 (1985)
79. D S Kummli, S Lobsiger, H-M Frey, S Leutwyler, J F Stanton *J. Phys. Chem. A* **112** 9134 (2008)
80. Z Chen, C S Wannere, C Corminboeuf, R Puchta, P von R Schleyer *Chem. Rev.* **105** 3842 (2005)
81. P von R Schleyer, C Maerker, A Dransfeld, H Jiao, N J R van E Hommes *J. Am. Chem. Soc.* **118** 6317 (1996)
82. G V Baryshnikov, B F Minaev, M Pittelkow, C B Nielsen, R Salcedo *J. Mol. Model.* **19** 847 (2013)
83. S Radenković, I Gutman, P Bultinck *J. Phys. Chem. A* **116** 9421 (2012)
84. T N Gribanova, N S Zefirov, V I Minkin *Dokl. Chem.* **426** 105 (2009) [*Dokl. Akad. Nauk* **426** 332 (2009)]
85. T N Gribanova, N S Zefirov, V I Minkin *Pure Appl. Chem.* **82** 1011 (2010)
86. R Krishnan, J S Binkley, R Seeger, J A Pople *J. Chem. Phys.* **72** 650 (1980)
87. L-W Shi, B Chen, J-H Zhou, T Zhang, Q Kang, M-B Chen *J. Phys. Chem. A* **112** 11724 (2008)
88. B Napolion, F Hagelberg, M-J Huang, J D Watts, T M Simeon, D Vereen, W L Walters, Q L Williams *J. Phys. Chem. A* **115** 8682 (2011)
89. T B Tai, V T T Huong, M T Nguyen *Chem. Commun.* **49** 11548 (2013)
90. G Monaco, P W Fowler, M Lillington, R Zanasi *Angew. Chem., Int. Ed.* **46** 1889 (2007)
91. J Aragó, P M Viruela, E Ortt *J. Mol. Struct. (THEOCHEM)* **912** 27 (2009)
92. T Ohmae, T Nishinaga, M Wu, M Iyoda *J. Am. Chem. Soc.* **132** 1066 (2010)
93. A Datta, S K Pati *J. Phys. Chem. C* **111** 4487 (2007)
94. G Gahungu, J Zhang, T Barancira *J. Phys. Chem. A* **113** 255 (2009)
95. T Fujimoto, M M Matsushita, H Yoshikawa, K Awaga *J. Am. Chem. Soc.* **130** 15790 (2008)
96. B F Minaev, G V Baryshnikov, V A Minaeva *Comput. Theor. Chem.* **972** 68 (2011)
97. V A Minaeva, B F Minaev, G V Baryshnikov, H Ågren, M Pittelkow *Vib. Spectrosc.* **61** 156 (2012)
98. V A Minaeva, B F Minaev, G V Baryshnikov, O M Romeyko, M Pittelkow *Vib. Spectrosc.* **65** 147 (2013)
99. V A Minaeva, B F Minaev, G V Baryshnikov, O N Romeyko, M Pittelkow *J. Appl. Spectrosc.* **79** 695 (2012) [*Zh. Prikl. Spektrosk.* **79** 709 (2012)]
100. V A Minaeva, B F Minaev, G V Baryshnikov, M Pittelkow *Opt. Spectrosc.* **114** 509 (2013) [*Opt. Spektroskop.* **114** 556 (2013)]
101. R R Valiev, V N Cherepanov *Int. J. Quant. Chem.* **113** 2563 (2013)
102. R R Valiev, H Fliegl, D Sundholm *J. Phys. Chem. A* **117** 9062 (2013)
103. G V Baryshnikov, R R Valiev, N N Karaush, B F Minaev *Phys. Chem. Chem. Phys.* **16** 15367 (2014)
104. T Nishinaga, T Ohmae, K Aita, M Takase, M Iyoda, T Arai, Y Kunugi *Chem. Commun.* **49** 5354 (2013)
105. W Jiang, Y Li, Z Wang *Chem. Soc. Rev.* **42** 6113 (2013)
106. O Vahtras, B Minaev, H Ågren *Chem. Phys. Lett.* **281** 186 (1997)
107. E R Andrew, A Bradbury, R G Eades *Nature (London)* **182** 1659 (1958)
108. V G Nenajdenko, V V Sumerin, K Yu Chernichenko, E S Balenkova *Org. Lett.* **6** 3437 (2004)
109. K Chernichenko, N Emelyanov, I Gridnev, V G Nenajdenko *Tetrahedron* **67** 6812 (2011)
110. A Yu Sokolov, D B Magers, J I Wu, W D Allen, P von R Schleyer, H F Schaefer III *J. Chem. Theory Comput.* **9** 4436 (2013)
111. R H Mitchell, P Zhang, D J Berg, R V Williams *Chem. Commun.* **48** 8144 (2012)
112. T Cao, Y Ma, X Yan, J Cheng, Y Luo, L He, W Zhu *Chin. J. Chem.* **27** 1914 (2009)
113. C Corminboeuf, T Heine, G Seifert, P von R Schleyer, J Weber *Phys. Chem. Chem. Phys.* **6** 273 (2004)
114. H Fallah-Bagher-Shaidaei, C S Wannere, C Corminboeuf, R Puchta, P von R Schleyer *Org. Lett.* **8** 863 (2006)
115. G Gahungu, J Zhang *Phys. Chem. Chem. Phys.* **10** 1743 (2008)
116. T K Dickens, R B Mallion *Phys. Chem. Chem. Phys.* **15** 8245 (2013)
117. C F Wilcox Jr, J P Uetrecht, K K Grohman *J. Am. Chem. Soc.* **94** 2532 (1972)
118. G V Baryshnikov, N N Karaush, B F Minaev *Chem. Heterocycl. Compd.* **50** 349 (2014) [*Khim. Geterotsikl. Soedin.* 381 (2014)]
119. I Willner, M Rabinovitz *J. Org. Chem.* **45** 1628 (1980)
120. K Aita, T Ohmae, M Takase, K Nomura, H Kimura, T Nishinaga *Org. Lett.* **15** 3522 (2013)
121. Y Shen, C-F Chen *Chem. Rev.* **112** 1463 (2012)
122. J H Dopper, D Oudman, H Wynberg *J. Org. Chem.* **40** 3398 (1975)
123. A Rajca, M Miyasaka, S Xiao, P J Boratyński, M Pink, S Rajca *J. Org. Chem.* **74** 9105 (2009)
124. A S Davydov *Teoriya Molekulyarnykh Eksitonov* (The Theory of Molecular Excitons) (Moscow; Nauka, 1968)
125. N N Karaush, B F Minaev, G V Baryshnikov, V A Minaeva *Opt. Spectrosc.* **116** 33 (2014) [*Opt. Spektroskop.* **16** 37 (2014)]
126. G Socrates *Infrared and Raman Characteristic Group Frequencies — Tables and Charts* (Chichester; Wiley, 2001)

127. J A Smith, M W George, J M Kelly *Coord. Chem. Rev.* **255** 2666 (2011)
128. V O Minaeva, B P Minaev, G V Barishnikov, I M Ozirna, M Pittel'kov *Visnik Cherkas'k. Univ., Ser. Khim. Nauki* (14) 32 (2013)
129. P L Polavarapu *J. Phys. Chem.* **94** 8106 (1990)
130. G Keresztury, S Holly, G Besenyei, J Varga, A Wang, J R Durig *Spectrochim. Acta, Part A* **49** 2007 (1993)
131. S Mohakud, S K Pati *J. Mater. Chem.* **19** 4356 (2009)
132. D Volyniuk, V Cherpak, P Stakhira, B Minaev, G Baryshnikov, M Chapran, A Tomkeviciene, J Keruckas, J V Grazulevicius *J. Phys. Chem. C* **117** 22538 (2013)
133. B Minaev, G Baryshnikov, H Ågren *Phys. Chem. Chem. Phys.* **16** 1719 (2014)
134. B Minaev, H Ågren, F De Angelis *Chem. Phys.* **358** 245 (2009)
135. E Jansson, B Minaev, S Schrader, H Ågren *Chem. Phys.* **333** 157 (2007)
136. B Minaev, V Minaeva, H Ågren *J. Phys. Chem. A* **113** 726 (2009)
137. X Li, B Minaev, H Ågren, H Tian *Eur. J. Inorg. Chem.* 2517 (2011)
138. X Li, B Minaev, H Ågren, H Tian *J. Phys. Chem. C* **115** 20724 (2011)
139. L Xiao, Z Chen, B Qu, J Luo, S Kong, Q Gong, J Kido *Adv. Mater.* **23** 926 (2011)
140. K Okumoto, Y Shirota *Chem. Mater.* **15** 699 (2003)
141. G V Baryshnikov, B F Minaev, N N Karaush, V A Minaeva *Phys. Chem. Chem. Phys.* **16** 6555 (2014)
142. G V Baryshnikov, B F Minaev, N N Karaush, V A Minaeva *RSC Adv.* **4** 25843 (2014)
143. T Lenosky, X Gonze, M Teter, V Elser *Nature (London)* **355** 333 (1992)
144. A Datta, S Mohakud, S K Pati *J. Mater. Chem.* **17** 1933 (2007)
145. V Mohan, A Datta *J. Phys. Chem. Lett.* **1** 136 (2010)
146. A Datta, S Mohakud, S K Pati *J. Chem. Phys.* **126** 144710 (2007)
147. B Szefler, M V Diudea *Molecules* **19** 15468 (2014)
148. J Yu, Q Sun, Y Kawazoe, P Jena *Nanoscale* **6** 14962 (2014)
149. W D Xiao, Y Y Zhang, L Tao, K Aït-Mansour, K Yu Chernichenko, V G Nenajdenko, P Ruffieux, S X Du, H-J Gao, R Fasel *Sci. Rep.* **4** 5415 (2014)
150. N N Karaush, G V Baryshnikov, B F Minaev *RSC Adv.* **5** 24299 (2015)
151. V T T Huong, T B Tai, M T Nguyen *RSC Adv.* **5** 24167 (2015)
152. S Nobusue, H Miyoshi, A Shimizu, I Hisaki, K Fukuda, M Nakano, Y Tobe *Angew. Chem., Int. Ed.* **54** 2090 (2015)
153. J Yin, K Chaitanya, X-H Ju *J. Mater. Chem. C* **3** 3372 (2015)
154. X Xiong, C-L Deng, B F Minaev, G V Baryshnikov, X-S Peng, H N C Wong *Chem. – Asian J.* **10** 969 (2015)